

Pollinator attractors: petaloidy and petal epidermal cell shape in close relatives of snapdragon

By

Copyright 2011

Jacob Brian Landis

Submitted to the graduate degree program in Ecology and Evolutionary Biology and the Graduate Faculty of the University of Kansas in partial fulfillment of the requirements for the degree of Master of Arts.

Chairperson Dr. Lena Hileman

Dr. Mark Mort

Dr. Paulyn Cartwright

Date Defended: April 13, 2011

The Thesis Committee for Jacob B Landis
certifies that this is the approved version of the following thesis:

Pollinator attractors: petaloidy and petal epidermal cell shape in close relatives of snapdragon

Chairperson Dr. Lena Hileman

Date approved: 30 June 2011

ABSTRACT

The diversity of angiosperms in floral form and development has been an area of interest for biologists. A multitude of studies investigating the evolution of flowering plants have attempted to determine why angiosperms are so diverse. One possible major contributor to flower form diversity is pollinator pressure. The interactions between flowers and their pollinators have important ecological and evolutionary consequences, with co-evolution often occurring. Many studies have looked at suites of floral traits that affect pollinator visitation, which have been coined pollination syndromes (Fenster et al., 2004). These traits include but are not limited to, flower color, flower orientation, landing platforms, and nectar guides.

With the increase in genetic tools, and the utilization of model species such as *Antirrhinum majus* (Plantaginaceae) and *Arabidopsis thaliana* (Brassicaceae), many studies are looking at the genetic architecture of floral traits. Studies have determined the genetic blueprint for floral organ identity, as well as in traits associated with pollination syndromes including flower color and symmetry. Using members of the Antirrhineae tribe (Plantaginaceae) makes it easier to effectively use the resources from *A. majus*, or snapdragon.

Chapter 1 investigates the applicability of the sliding boundary model for petaloid sepal formation in *Rhodochiton atrosanguineum*, a close relative of snapdragon. We were interested in determining if the petaloid sepals of *R. atrosanguineum* had true petal identity, or were merely just colorful sepals. Chapter 2 focuses on possible petal function, and not merely petal identity. Conical cells are found on roughly 80% of angiosperms (Kay et al., 1981) and are thought to be a marker for petal identity. However, conical cells are thought to be absent mostly in hummingbird pollinated flowers, though no studies have looked at this in depth (Christensen and Hansen, 1998). For this chapter, we investigated possible correlated evolution between petal epidermal cell shape and pollination system.

ACKNOWLEDGEMENTS

There are many people, institutions, and groups that I would like to thank for making this all possible. First I would like to thank my Masters advisor Lena Hileman. She has been a major influence in allowing me to gain the experience and skills, as well as supplying the tools and equipment, that have gotten me to where I am today. I would also like to thank Mark Mort and Paulyn Cartwright for being on my committee and helping me make sure I stayed on the path in order to get things accomplished. Past and current members of the Hileman lab deserve thanks for helping with lab work, especially Jill Preston, Laryssa Barnett, Kima Scott, and Bethany Wright.

I would not have been able to complete this work without help from outside the lab including David Moore and the imaging facility at KU for helping obtain images of my plants and to figure out what to do with them, as well as Katie Sadler and the rest of the greenhouse for helping keep plants alive and flowering for the last several years. I would like to thank the Botany Endowment and the Department of Ecology and Evolutionary Biology for funding opportunities for both research and the ability to attend national conferences to present my work.

Lastly, I would like to thank my friends and family for being supportive through this process. Many of you have given great advice through the difficulties, as well as lending a sympathetic ear when things weren't going right. For all of which I am greatly thankful.

TABLE OF CONTENTS

Title Page	i
Acceptance page.....	ii
Abstract	1
Acknowledgements	2
Table of Contents	3
Chapter 1. A test of the sliding boundary model in petaloid sepals of <i>Rhodochiton</i>	
<i>atrosanguineum</i> (Plantaginaceae), a close relative of snapdragon	
Abstract	5
Introduction	6
Methods	9
Results	13
Discussion	16
Chapter 2. The birds and the bees: testing for correlated evolution between petal cell shape and	
pollinators.	
Abstract	21
Introduction	22
Methods	25
Results	31
Discussion	37
<u>List of Figures</u>	
Figure 1. Phylogeny of Antirrhineae	9
Figure 2. Scanning Electron Microscope images of sepals and petals	14
Figure 3. Gene tree of <i>DEFICIENS</i> and <i>GLOBOSA</i>	15

Figure 4. RT-PCR expression patterns of <i>DEFICIENS</i> and <i>GLOBOSA</i>	17
Figure 5. <i>in situ</i> hybridization images of <i>DEFICIENS</i> and <i>GLOBOSA</i>	17
Figure 6. ITS Phylogeny of Antirrhineae	32
Figure 7. Phylogenetic mapping of pollinator system and petal cell shape	33
Figure 8. Height/width ratios of cells on dorsal and ventral petal lobes	34
Figure 9. Examples of conical and non-conical cells	35
Figure 10. Transition rates between pollinator types and cell shape	36
Figure 11. Gene tree of four orthologs of <i>MIXTA-LIKE</i> genes	38

List of Tables

Table 1. Taxa included in study, seed stocks, GenBank accession numbers and accession numbers to Herbarium	25
Table 2. Taxa included, inferred pollination system, and references	28
References	44

List of Appendices

Appendix 1. GenBank accession numbers for B-class genes	60
Appendix 2. GenBank accession numbers for <i>MIXTA-LIKE</i> genes	61

A test of the sliding boundary model in petaloid sepals of *Rhodochiton atrosanguineum* (Plantaginaceae), a close relative of snapdragon

ABSTRACT

This study investigates whether the outer whorl organs of *Rhodochiton atrosanguineum* flowers, which superficially appear petaloid, exhibit characteristics of petals at both the micromorphological and developmental genetic level. The hypothesized ABC genetic model explains organ identity development for most core eudicot flowers, while for those with multiple petaloid organs the hypothesized sliding boundary model is often more appropriate. The sliding boundary model states expansion of B-function in the outer whorl perianth will specify petaloid sepals. This study tests whether the sliding boundary model applies in *R. atrosanguineum*. Scanning electron micrographs were generated to determine whether petaloid sepals exhibit micromorphological characteristics of petals. To test the applicability of the sliding boundary model hypothesis, we examined the expression of B-class MADS box genes during flower development using both reverse-transcriptase PCR and in situ mRNA hybridization. We show that epidermal cell shape of outer whorl petaloid sepals is inconsistent with petal identity in these organs. In addition, we establish that B-class gene expression is restricted to the second and third floral whorls, consistent with the original formulation of the ABC model, not the sliding boundary model. From our data, we conclude that petaloid sepals of *R. atrosanguineum* lack both petal epidermal cell identity and petal identity resulting from B-class gene function, leaving other candidate genes likely responsible for their petaloid appearance. This study, in conjunction with other studies not supporting the sliding boundary model, suggests multiple convergent pathways in the evolution of showy sepals.

INTRODUCTION

Angiosperm flowers show a wide range of diversity, much of which can be attributed to evolutionary changes in the size, shape, number and color of petal or petaloid organs, which function to attract pollinators. Petal evolution has been suggested to involve multiple originations (Zanis et al., 2003; De Craene, 2007; Rasmussen et al., 2009; Soltis et al., 2009,) as well as multiple losses of petals also being documented (Jaramillo and Kramer, 2007; Wu et al., 2007). Indeed, in some cases, such as, but not limited to, the genus *Cornus*, other floral and extrafloral organs, including bracts, have evolved petal identity (Geuten, 2006; Maturen, 2008; Zhang et al., 2008; Brockington, 2009; Rasmussen et al. 2009).

The typical core eudicot flower consists of four concentric whorls of floral organs. The two outer-most whorls of organs develop into a differentiated perianth surrounding the reproductive organs. In this typical flower, leaf-like sepals develop in the outer perianth whorl, and petals occupy the inner perianth whorl. Petals are often highly complex and are morphologically separate from leaves and sepals due to several characteristics, including the presence of colored pigmentation, conical or elongated epidermal cell shapes, lack of stomata, and lack of palisade mesophyll (reviewed in Glover, 2007; De Craene, 2008; Irish, 2009). Another characteristic that distinguishes petals from sepals and leaves is the necessary gene products for petal specification (reviewed in Irish, 2009). Interestingly, many angiosperms develop flowers which do not conform to the typical form described above – most notably, those in which all perianth organs exhibit a petaloid appearance (*e.g.*, orchids, lilies, columbines, magnolias; reviewed in Kramer, 2007; Litt and Kramer, 2010), and the extent to which outer whorl perianth organs adopt petal identity has been studied in multiple taxa (Kanno et al., 2003; Park, 2004; Nakamura et al., 2005; Geuten et al., 2006; Maturen, 2008).

For the typical flower with a differentiated perianth, the ABC model posits that the combination of three classes of genes, termed A, B, and C, function in overlapping domains to specify the formation of the different floral organ identities (Schwarz-Sommer et al. 1990; Bowman et al. 1991; Coen et al. 1991; Coen and Meyerowitz 1991; Trobner et al. 1992). Presence of A-class function determines sepals in the outer whorl, with co-occurrence of A- and B-class function determining petal identity in the second whorl. Stamens are determined in the third whorl by co-occurrence of B- and C-class function, and in the fourth whorl, occurrence of C-class function determines the identity of carpels. Therefore, based on the ABC model, B-class proteins play a critical developmental role in establishing petal identity, and in the differentiation of petal from sepal identity within the perianth.

B-class genes comprise two lineages: the *APETALA3/DEFICIENS* lineage (Sommer et al., 1990; Jack et al., 1992) and the *PISTILATA/GLOBOSA* lineage (Trobner et al. 1992; Goto and Meyerowitz 1994). Since their original characterization in *Arabidopsis thaliana* L. (Brassicaceae) and *Antirrhinum majus* L. (Plantaginaceae) (Bowman et al., 1989; Carpenter and Coen, 1990; Schwarz-Sommer et al., 1990; Sommer et al., 1990; Krizek and Meyerowitz, 1996) many additional studies have demonstrated that B-class function in establishing petal identity is conserved in the angiosperms including flowering tobacco (*Nicotiana benthamiana* Domin, Solanaceae; Liu et al. 2004), tomato (*Solanum lycopersicum* L., Solanaceae; de Martino et al. 2006), petunia (*Petunia hybrida* Juss., Solanaceae; Rijpkema et al. 2006; Vandenbussche et al., 2004), poppy (*Papaver somniferum* L., Papaveraceae; Drea et al., 2007), rice (*Oryza sativa* L., Poaceae; Kang et al. 1998; Prasad and Vijayraghavan 2003; Xiao et al. 2003), and maize (*Zea mays* L., Poaceae; Ambrose et al. 2000; Whipple et al., 2004).

As mentioned earlier, many core eudicot species develop perianths that are undifferentiated or exhibit reduced differentiation. Phenotypically in these species, the ABC

model does not appear to be fully applicable. To explain the developmental genetic program underlying these types of flowers, the sliding boundary model was developed (Bowman, 1997; Kramer et al., 2003). According to this model, A- and B-class function in both the inner and outer whorl perianth organs leads to an expansion of petal identity across the entire perianth. Data from multiple species, including columbine (*Aquilegia vulgaris* L., Ranunculaceae; Kramer et al., 2007), tulip (*Tulipa gesneriana* L., Liliaceae; Kanno et al., 2003), lily (*Lilium longiflorum* Thunb., Liliaceae; Tzeng and Yang, 2001), lily of the Nile (*Agapanthus praecox* Willd., Alliaceae; Nakamura et al., 2005) and water lilies (*Najas caroliniana* Gray, Cabombaceae; Yoo et al., 2010) support the sliding boundary model as an explanation for the presence of an entirely petaloid perianth. However, in other species the sliding boundary model does not explain petal identity in outer whorl perianth organs as documented in common heather (*Calluna vulgaris* (L.) Hull, Ericaceae; Borchert et al., 2009), gerbera (*Gerbera hybrida* L., Asteraceae; Broholm et al., 2010), orchids (*Habenaria radiata* (Thunb.) Spreng., Orchidaceae; Kim et al., 2007), impatiens (*Impatiens hawkeri* W. Bull, Balsaminaceae; Geuten et al., 2006), and garden asparagus (*Asparagus officinalis* L., Asparagaceae; Park et al., 2003; Park et al., 2004).

The focus of this study is *Rhodochiton atrosanguineum* L. (Plantaginaceae), a close relative of the model species snapdragon (Fig 1a). *Rhodochiton atrosanguineum* flowers do not phenotypically adhere to the ABC model in the same fashion as snapdragon flowers with their distinct sepals and petals (Fig. 1b). *Rhodochiton atrosanguineum* flowers have outer and inner whorl perianth organs that are morphologically distinct, but unlike snapdragon flowers both whorls of organs exhibit a petaloid appearance (Fig 1c). In this study we aim to determine the extent to which outer whorl perianth organs of *R. atrosanguineum* exhibit petal identity beyond pigmentation of their sepals. Therefore, we investigate perianth micromorphology with the specific hypothesis that *R. atrosanguineum* outer whorl perianth organs will exhibit

characteristics of epidermal cell shape resembling inner whorl petals. We also test the applicability of the sliding boundary model, with the specific prediction that expression of B-class orthologs *DEF* and *GLO* will be detected in *R. atrosanguineum* outer whorl perianth organs if they have adopted petal identity.

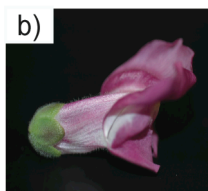
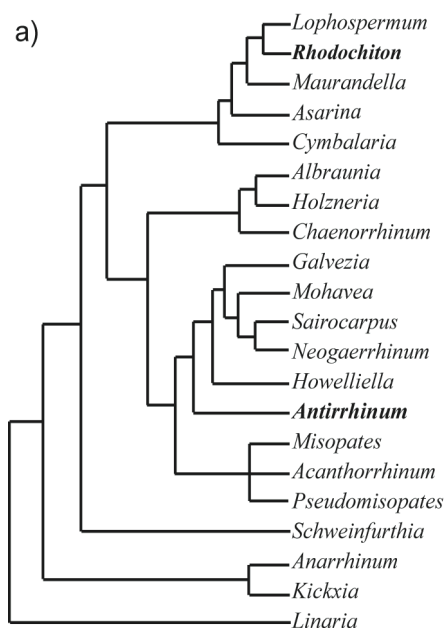


Figure 1. Phylogenetic context of study species. a) ITS phylogeny adapted from Vargas et al. (2004) showing relationships within the tribe Antirrhineae (Plantaginaceae). Focal genera *Rhodochiton* and *Antirrhinum* are bold faced to exemplify their relationship to each other. b) *Antirrhinum majus* (snapdragon) with showy pink petals and leaf-like sepals. c) *Rhodochiton atrosanguineum* with petaloid sepals.

METHODS

Plant material- Seeds of *R. atrosanguineum* were obtained from B and T World Seeds (<http://www.b-and-t-world-seeds.com>) and *A. majus* seeds, accession number ANTI 11 (D2836), were obtained from the Gatersleben collection (Leibniz Institute of Plant Genetics and Crop Research, <http://www.ipk-gaterlsehen.de>). Voucher specimens of *R. atrosanguineum* (JL001 and JL002) and *A. majus* (JL004) have been placed in the R. L. McGregor Herbarium (KANU), University of Kansas. Flower material for both species was collected from plants grown in the greenhouse at the University of Kansas.

Scanning electron microscopy- Mature flowers of *A. majus* and *R. atrosanguineum* were fixed in glutaraldehyde (5% glutaraldehyde solution in 0.1 M phosphate buffer) overnight

and then dehydrated through an ethanol series. Dehydrated flowers were critical point dried using a Tousimis critical point dryer and then dissected into sepals, base of petal tube, and petal lobe. Tissue was collected for imaging both adaxial and abaxial surfaces. Specimens were mounted on stubs, sputter-coated with gold, and viewed with a D. Leo field emission scanning electron microscope.

Isolation of *RaDEF* and *RaGLO* orthologs- Total RNA was isolated from immature *R. atrosanguineum* flowers using Trizol following the manufacturer instructions (Ambion, Austin, Texas, USA) and DNase treated using TurboDNA (Ambion, Austin, Texas, USA). cDNA was generated using 1 µg of total RNA in a 15 µl cDNA synthesis reaction using iScript Synthesis Kit following the manufacturer instructions (BioRad, Hercules, California, USA). Orthologs of *DEF* and *GLO* were isolated from floral cDNA by reverse-transcriptase PCR (RT-PCR) using the degenerative forward primer (5'-AACAGGCARCTIACITAYTC-3') and the reverse PolyT-QT primer (5'-GACTCGAGTCGACATGGA(T)₁₈-3') (Hileman et al. 2006). This primer combination yields full length gene sequences minus 21 amino acids on the 5' end. RT-PCR reactions contained 2 ul of 1:10 diluted cDNA, 1.25 units *Taq* (Sigma-Aldrich, St. Louis, Missouri, USA), 10X PCR buffer, 0.5 µM of each primer, and 0.8 mM dNTPs. PCR reactions were run for 40 cycles with an annealing temperature of 47°C. PCR products were subjected to gel electrophoresis using a 1.5% agarose gel and gel-purified using the Wizard SV Gel and PCR Clean Up System Kit (Promega, Madison, Wisconsin, USA) before being cloned. Gel-purified PCR products were cloned into the pGEM -T vector system (Promega, Madison, Wisconsin, USA) following the manufacturer instructions. Twenty clones were sequenced using M13 forward and M13 reverse primers in order to identify multiple gene copies amplified by our RT-PCR approach (Howarth and Baum, 2005).

Phylogenetic Analysis- Putative orthologs of *RaDEF* and *RaGLO* were aligned to additional B-class (*DEF/GLO*-like) genes downloaded from Genbank (Appendix 1) using MUSCLE (Edgar, 2004), followed by manual adjustment in MacClade v4.08 (Maddison and Maddison, 2005). Nucleotide sequence alignments were used to generate estimates of the gene phylogeny under Maximum Parsimony (MP), Maximum Likelihood (ML) and Bayesian criteria. Maximum likelihood was implemented in Garli (Zwickl, 2006) using the GTR + I + Γ model of molecular evolution. Support values using ML were generated with 1000 bootstrap replicates in Garli as described above. Support values were also generated using MP in Paup* 4.0 (Swofford 2002) with 1000 heuristic bootstrap replicates and the TBR branch swapping algorithm. Bayesian criterion was implemented using MrBayes (Huelsenbeck and Ronquist, 2001; Ronquist and Huelsenbeck, 2003) and the GTR + I + Γ model of molecular evolution with two Markov chains running for 1,000,000 generations sampling every 100th generation. At completion of runs, the two chains were checked for convergence and the first 25% of saved trees were discarded as initial burn-in. Remaining trees were used to calculate posterior probabilities of node support in a 50% majority-rule consensus tree.

Expression of *RaDEF* and *RaGLO* by Reverse Transcriptase (RT)-PCR-

Rhodochiton atrosanguineum RNA was extracted and cDNA generated from the four floral organs of multiple flowers: outer-whorl petaloid sepals, petals, stamens and carpels, in three distinct floral size classes as described above. The small size class included the earliest stage flower buds that could be hand-dissected, and corolla length in this size class ranged from 4.0 to 7.0 mm. Corolla length in the medium size class ranged from 15.0 to 18.0 mm. The large size class included flowers just pre-anthesis, and corolla length in this size class ranged from 39.5 to 40.5 mm. Expression patterns were characterized using gene specific primers designed to amplify fragments of *RaDEF* and *RaGLO* of ca. 150-200 bp of the open reading frame. Gene

specific primers for amplifying *RaDEF* were *RaDEF-F* (5'-AGCTTGAACGATCTGGGCTA-3') and *RaDEF-R* (5'-GTGCGGATCCTCTCTTCTTG-3'), and primers for amplifying *RaGLO* were *RaGLO-F* (5'-GGGACGTCAGCTCTCAAAA-3') and *RaGLO-R* (5'-ATCGTATAACCCCTGGCTTT-3'). *ACTIN* was used as a loading control as described in Prasad et al. (2001). RT-PCR reactions included 2 µl of 1:10 diluted cDNA, 1.25 units *Taq* (Sigma-Aldrich, St. Louis, Missouri, USA), 10X PCR buffer, 0.5 µM of each primer, and 0.8 mM dNTPs. PCR conditions consisted of 26 cycles with an annealing temperature of 55°C for all genes tested. The number of cycles was determined as that representing the linear range of amplification from a PCR product curve including reactions run for 22-40 cycles. Triplicate RT-PCR reactions for each cDNA, including RT-PCR negative control cDNAs (-RT), were conducted to ensure consistency.

Expression of RaDEF and RaGLO by in situ mRNA hybridization- Flower buds of *R. atrosanguineum* were fixed in FAA (47.5% ethanol, 5% acetic acid, 3.7% formaldehyde) for 8 hours, stained with eosin Y, dehydrated and wax embedded as described in Jackson (1991) and Preston and Kellogg (2007). Gene specific probe templates of *RaDEF* and *RaGLO* were generated using primers *RaDEF-F* (5'-AATACATCAGTCCCACCACAGC-3'), *RaDEF-R* (5'-GCAAAGCAAATGTGGTAAGGTC-3'), *RaGLO-F* (5'-TCATCATCTTTGCTAGTTCTG-3'), and *RaGLO-R* (5'-TCCTGAAGATTAGGCTGCATTG-3'). Probes were 520 bp and 488 bp long for *RaDEF* and *RaGLO* respectively, with forward primers in the I domain and reverse primers in the C-terminal coding region of each gene (Yang et al. 2003), to exclude amplification of the highly conserved MADS domain. All PCR products for probe generation were cloned into the pGEM -T vector (Promega, Madison, Wisconsin, USA) and confirmed by sequencing. Sense and antisense riboprobes for *RaDEF* and *RaGLO* were generated using T7 and SP6 RNA polymerase (Roche, Indianapolis, Indiana, USA) incorporating digoxigenin dNTPs (Roche, Indianapolis,

Indiana, USA) according to the manufacturers instructions. Probe hydrolysis followed Jackson (1991) to yield fragments c. 150 bp long. In situ hybridization was performed on longitudinal sections of multiple inflorescences as in Jackson (1991). Images were documented using a Leica DM5000B microscope attached to a Leica DFC300FX camera. Images were imported into Adobe Photoshop and adjusted for contrast, brightness and color balance.

RESULTS

Micromorphological analysis of petaloid sepals- To determine whether *R. atrosanguineum* petaloid sepals exhibit micromorphological cell shape characteristics found in *R. atrosanguineum* petals, SEM analyses were undertaken. Figure 2 shows image comparisons of epidermal cell shape from both the abaxial and adaxial surface of snapdragon (Fig. 2a-h) and *R. atrosanguineum* (Fig. 2i-p) leaves, sepals or petaloid sepals, and petals. Leaves (Fig. 2a,e,i,m), sepals and petaloid sepals (Fig. 2b,f,j,n) of both species show a consistent jigsaw-shaped cellular pattern on both the abaxial and adaxial surfaces, with stomata found predominantly on the abaxial surface of these organs (Fig. 2a,b,i,j). Jigsaw-shaped cells are also observed on the abaxial surface of both snapdragon and *R. atrosanguineum* petal lobes (Fig. 2d, l); interestingly, stomata are also found on the abaxial surface of *R. atrosanguineum* petal lobes (Fig. 2l), but not the abaxial surface of snapdragon petal lobes (Fig. 2d). *Rhodochiton atrosanguineum* abaxial petal lobe epidermal cells not only develop stomata but also appear more domed, or lenticular, than corresponding snapdragon epidermal cells (Fig. 2d,l). In both species, elongated cells were found on both adaxial and abaxial surfaces at the base of the corolla tube (Fig. 2c,g,k,o). The major difference between the two species is found on the surface of adaxial petal lobes. The adaxial surface of *A. majus* petal lobes (Fig. 2h) exhibit papillose conical cells as previously documented (Noda et al., 1994; Perez-Rodriguez et al., 2005), while the adaxial petal lobes of *R. atrosanguineum* (Fig 2p) lack conical cells. *Rhodochiton*

atrosanguineum adaxial petal lobe epidermal cells are more domed than the papillose conical epidermal cells found in snapdragon, and are referred to as lenticular (Kay, 1981). SEM images show no distinct micromorphological differences between petaloid sepals and leaf like sepals of *R. atrosanguineum* and snapdragon, respectively, and *R. atrosanguineum* petaloid sepals do not resemble *R. atrosanguineum* petals at the micromorphological scale.

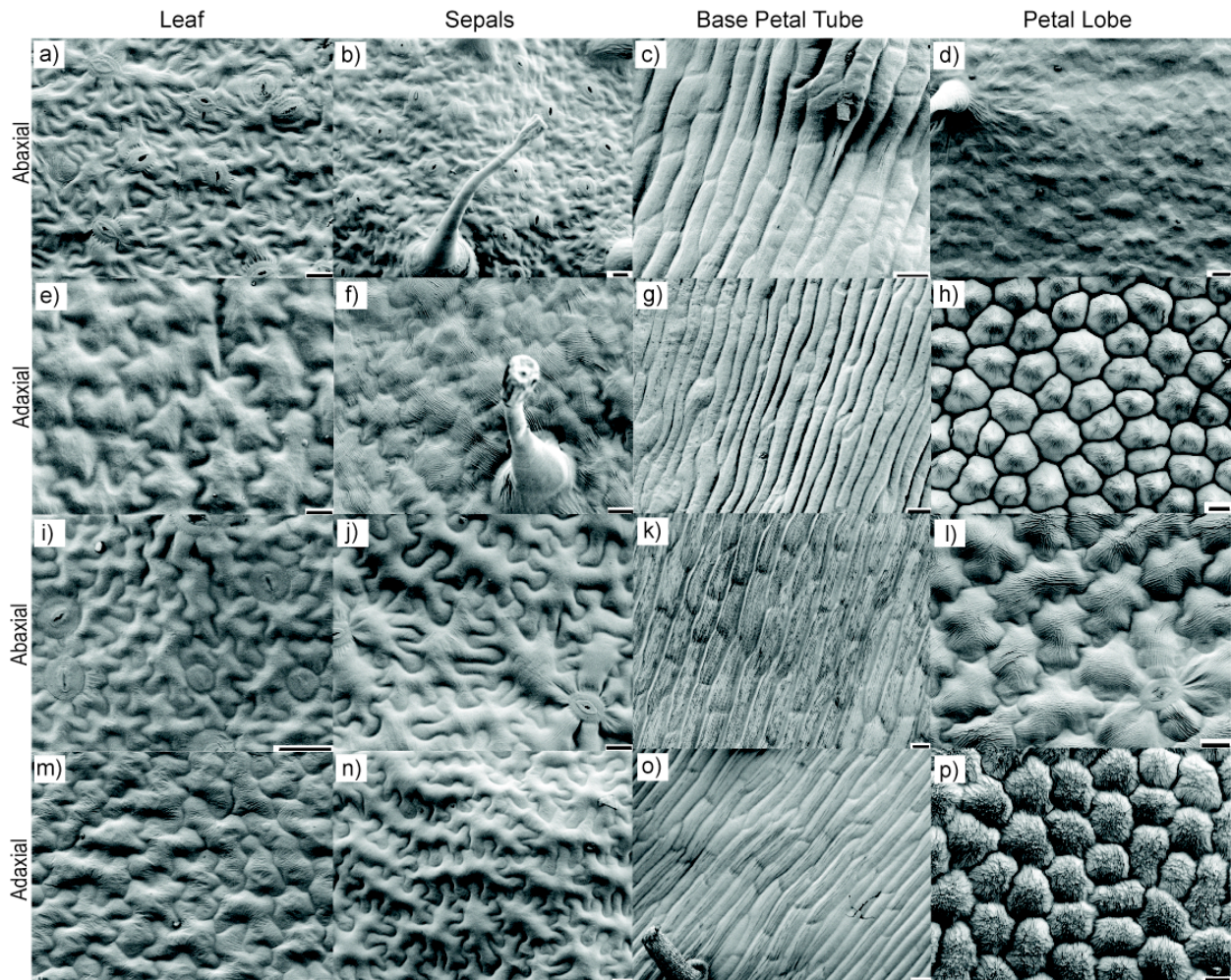


Figure 2. Scanning electron microscope (SEM) images from *Antirrhinum majus* (snapdragon; a-h) and *Rhodochiton atrosanguineum* (i-p). Individual SEM images of *A. majus* are a) abaxial leaf, b) abaxial sepal, c) abaxial base of petal tube, d) abaxial petal lobe, e) adaxial leaf, f) adaxial sepal, g) adaxial base of petal tube, h) adaxial petal lobe. Individual SEM images of *R. atrosanguineum* are i) abaxial leaf, j) abaxial sepal, k) abaxial base of petal tube, l) abaxial petal lobe, m) adaxial leaf, n) adaxial sepal, o) adaxial base of petal tube, p) adaxial petal lobe. Images show conserved jig-saw shaped patterns of cell shape in leaves and sepals of the two species, and conserved elongated tubular cells at the base of the petal tube between both species. *Rhodochiton atrosanguineum* lacks conical cells on the adaxial surface of the petal lobe as seen in snapdragon, whereas the abaxial petal lobe of *R. atrosanguineum* has a more defined cell shape than those seen in snapdragon. Scale bars in c, g, o are 30 μm , all others are 20 μm .

Isolation and phylogenetic assessment of *RaDEF* and *RaGLO*- Two B-class genes were isolated from floral cDNA of *R. atrosanguineum*. ML, MP and Bayesian phylogenetic estimates place one of these two genes (*RaDEF*) in a well-supported clade with *A. majus DEF*, and the other gene (*RaGLO*) in a clade with *A. majus GLO* (Fig. 3). *RaDEF* is nested within a clade of orthologs from snapdragon and *Misopates orontium* (L.) Raf. (Plantaginaceae), all of which are members of the Antirrhineae. This clade has bootstrap support values of 97% (MP) and 98% (ML), and a posterior probability of 1.0 (Fig. 3). The placement of *RaGLO* is also in a well-supported clade with *GLO*-like genes from snapdragon and *M. orontium* with bootstrap values of 100% (MP) and 90% (ML) and a posterior probability of 1.0 (Fig. 3). The sister relationship between snapdragon and *M. orontium* is highly supported and reflects species relationships based on other molecular markers (Vargas et al., 2004).

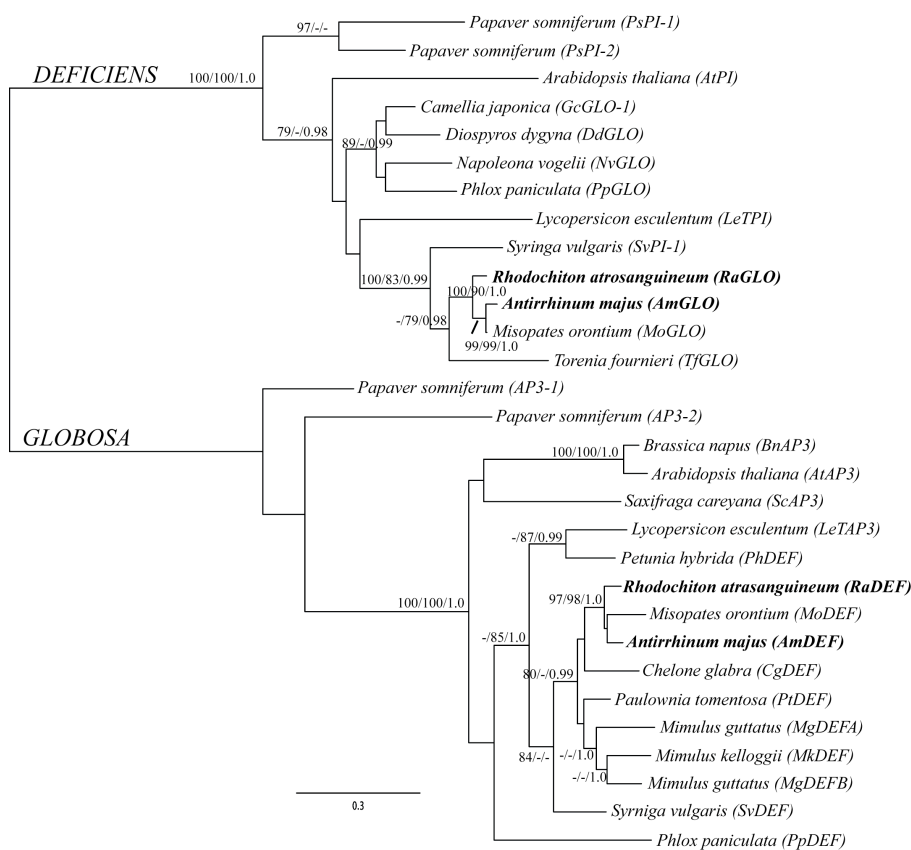


Figure 3. Phylogeny of *DEFICIENS* (*DEF*) and *GLOBOSA* (*GLO*) orthologs showing placement of newly sequenced *Rhodochiton atrosanguineum DEF* and *GLO*. Shown is the maximum-likelihood (ML) tree with support values from 1000 replicate Maximum Parsimony bootstrap analysis/1000 replicate ML bootstrap analysis/Bayesian posterior probabilities. Only support values of >75% for bootstrap and >0.95 Bayesian posterior probabilities are shown on the phylogeny.

Expression of *RaDEF* and *RaGLO*- Scoring of RT-PCR gene expression was dichotomous – presence or absence of *RaDEF* or *RaGLO* transcripts in sampled tissues. *RaDEF* and *RaGLO* transcripts were detected by RT-PCR in petals and stamens, but not in petaloid sepals or carpels, for the three size classes of flowers (Fig. 4). Expression of *ACTIN* was detected by RT-PCR in all sampled tissues at levels similar to *RaDEF* and *RaGLO* in petals and stamens, establishing that the absence of PCR product in *R. atrosanguineum* petaloid sepals and carpels was not due to insufficient template cDNA. These results demonstrate that, at least in later stages of flower development, the B-class genes, *RaDEF* and *RaGLO*, are not expressed in *R. atrosanguineum* petaloid sepals.

RaDEF and *RaGLO* expression was determined in earlier stage flowers by in situ mRNA hybridization. Anti-sense gene-specific probes for *RaDEF* (Fig. 5a) and *RaGLO* (Fig. 5c) show dark blue staining in the early forming petals and stamens. *RaDEF* (Fig. 5b) and *RaGLO* (Fig. 5d) gene-specific sense probes show no dark blue staining anywhere on the flower bud and serve as negative controls by establishing the amount of background staining that occurred during the in situ protocol. Multiple floral sections hybridized with antisense or sense probe were visualized to ensure consistent assessment of gene expression. Hybridization with antisense probes demonstrates that even at very early stages of flower development, *RaDEF* and *RaGLO* expression is restricted to the petal and stamen whorls.

DISCUSSION

Rhodochiton atrosanguineum sepals are brightly pigmented giving them a superficial petaloid appearance (Fig. 1c). The objective of this study was to determine to what extent *R. atrosanguineum* petaloid sepals have adopted petal characteristics at the micromorphological and molecular level. Specifically, we used SEM and gene expression studies to test the following hypotheses: 1) *R. atrosanguineum* petaloid sepals exhibit micromorphological characteristics

found in adjacent petals, and 2) the sliding boundary model applies to the development of petaloid sepals in *R. atrosanguineum*. We found that petaloid sepals of *R. atrosanguineum* do not morphologically resemble the petals of *R. atrosanguineum*, similar to what was found in impatiens (Geuten et al., 2006). Secondly, we found that the sliding boundary model does not apply to the development of petaloid sepals in *R. atrosanguineum*.

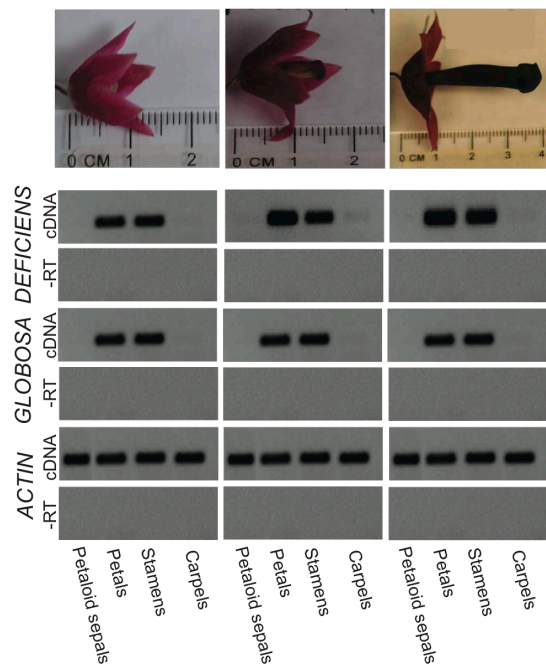


Figure 4. RT-PCR conducted on cDNA generated from three size classes of *R. atrosanguineum* flowers separated into their four floral organs. Small class flowers had a corolla length ranging from 4-7 mm, medium class flowers had a corolla length ranging from 15-18 mm, with large class flowers having corolla lengths of 39.5-40.5 mm. For all size classes, *DEFICIENS* and *GLOBOSA* were only expressed in the petals and stamens as seen by presence of bands in these organs. *ACTIN* was used as a loading control during RT-PCR analysis to insure the integrity cDNA. -RT samples served as negative controls, and no bands were visible in these reactions. *ACTIN* was also tested to show integrity of cDNA.

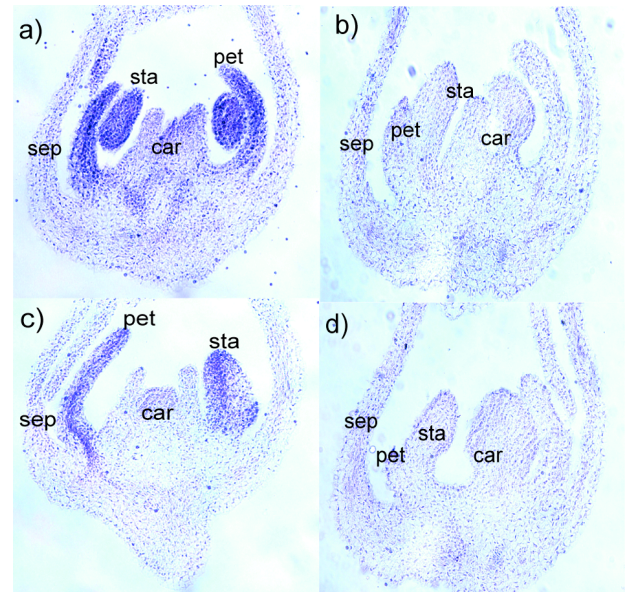


Figure 5. *In situ* hybridization conducted on early stage flower buds of *R. atrosanguineum*. a) Expression of *RaDEF* using antisense probe. b) Sense probe control for *RaDEF*. c) Expression of *RaGLO* using antisense probe. d) Sense probe control for *RaGLO*. Dark blue staining using antisense probes for *RaDEF* and *RaGLO* show that expression of these genes is limited to the developing petals and stamens of *R. atrosanguineum*. Petaloid sepals = sep, petals = pet, stamens = sta, and carpels = car.

If, in *R. atrosanguineum*, the sepals are petaloid in appearance due to an expansion of petal identity, then we expect epidermal cell shape in these outer whorl organs to resemble epidermal cell shapes found in petals. *Rhodochiton atrosanguineum* petaloid sepals develop

jigsaw shaped cells, very similar to the cells found in sepals of snapdragon (Figs. 2b and 2j). These jigsaw shaped cells are distinct from the adaxial epidermal cells of *R. atrosanguineum* petals (Figs. 2h and 2p), which are dome-shaped and distinguish petals at the micromorphological level from *R. atrosanguineum* petaloid sepals and leaves.

It is noteworthy that conical or papillose cell shape is found on the adaxial surface of many flowering plant species (Kay, 1981; Christensen and Hansen, 1998; Whitney and Glover, 2007; De Craene, 2008), but these predicted papillose cells were found only on the adaxial epidermis of snapdragon petals as previously described (Noda et al., 1994; Perez-Rodriguez et al., 2005) (Fig. 2h). Cell micromorphology of *R. atrosanguineum* petal lobes is drastically different than snapdragon (Figs. 2h and 2p). Not only are stomata found on the abaxial surface of *R. atrosanguineum* petals (Fig. 2l), which is rarely observed in flowering plants (De Craene, 2008), but also *R. atrosanguineum* adaxial petal surfaces lack the distinctive papillose conical cells found in snapdragon and many other species (Noda et al., 1994; Perez-Rodriguez et al., 2005). The ultimate cause of differences between *R. atrosanguineum* and snapdragon petals is unknown, but may reflect differences in pollination syndrome between the two species. Snapdragon is bee pollinated (Glover and Martin, 1998; Whitney et al., 2009) while *R. atrosanguineum* is pollinated by hummingbirds (Sutton, 1988). Differences in petal micromorphological characteristics may reflect evolutionary shifts in biotic or abiotic pollination mechanisms (Cronk and Ojeda, 2008; Di Stilio, 2010).

A single copy of *DEF* and *GLO* were identified in *R. atrosanguineum* and, based on our phylogenetic estimates (Fig. 3), are considered orthologous to *DEF* and *GLO* from snapdragon. RT-PCR analyses show that both *RaDEF* and *RaGLO* expression is restricted to the petals and stamens in mid to late-stage flower buds of *R. atrosanguineum* (Fig. 4). Similarly, at very early stages of flower development, in situ hybridization experiments show that *RaDEF* and *RaGLO*

expression is restricted to the petal and stamen whorls (Fig. 5). In conjunction, both approaches demonstrate that expansion of B-class gene expression to outer whorl perianth organs, as predicted by the sliding boundary model (Kramer et al., 2003), is not responsible for the petaloid appearance of *R. atrosanguineum* sepals. This study joins other studies showing that in some cases the sliding boundary model does not explain the development of petaloid sepals (Park et al., 2004; Geuten et al., 2006; Kim et al., 2007; Borchert et al., 2009; Broholm et al., 2010). Although *R. atrosanguineum* outer whorl organs are petaloid in appearance, they are morphologically quite distinct from the inner whorl petals (Fig. 1c), suggesting that changes in the anthocyanin pathway (Weiss, 2000; Whittall et al., 2006) may underlie the evolution of petal-like sepals in *R. atrosanguineum*.

Clearly convergent mechanisms are present leading to the formation of petaloid sepals, and may involve evolutionary changes at the level of B-class gene expression, upstream or downstream of B-class genes, or parallel pathways (Jaramillo and Kramer, 2004; Kramer et al., 2007; Litt and Kramer, 2010). Interestingly *R. atrosanguineum* exhibits a bipartite perianth (Fig. 1c) common to core eudicots, lacks duplicates of *DEF* and *GLO*, and gene expression data from this species does not support the sliding boundary model. Because B-class genes play a critical role in establishing a bipartite perianth, constraints are likely present for the evolution of petaloid sepals by mechanisms involving B-class genes (Kramer et al., 2003; reviewed in Hileman and Irish, 2009). Strikingly, when the sliding boundary model is supported it is restricted to species that have a history of gene duplications in *DEF* and/or *GLO* lineages, or lack a differentiated perianth (Tzeng and Yang, 2001; Kanno et al., 2003; Nakamura et al., 2005; Kramer et al., 2007; Litt and Kramer, 2010; Yoo et al., 2010). This study provides support for the emerging pattern that there are multiple, convergent developmental genetic mechanisms underlying independent transitions to petaloidy in the outer whorl perianth, and that constraint lies, at least in part, in

whether there is morphological differentiation within the perianth, and whether there is a history of duplication in the B-class gene lineage.

The birds and the bees: testing for correlated evolution between petal cell shape and pollinators

ABSTRACT

The interactions between flowers and their pollinators have important ecological and evolutionary consequences. Many studies have looked at suites of floral traits that affect pollinator visitation, which have been coined pollination syndromes. These traits include but are not limited to, flower color, flower orientation, landing platforms, and nectar guides. One trait that has not been looked at in great detail is petal epidermal cell shape. For this study we tested the hypothesis of correlated evolution between pollinators and petal epidermal cell shape. To accomplish this we focused on the tribe Antirrhineae, which contains 28 genera and roughly 300 species, most notably *Antirrhinum majus*, commonly known as snapdragon. For 17 species representing 15 genera, pollinators and presence/absence of conical cells on the dorsal and ventral petal lobes were coded as binary characters and mapped on to a phylogeny. We identified three independent transitions from bee pollination to hummingbird pollination. Also observed were three independent transitions of conical to non-conical cells in dorsal petal lobes, and two similar transitions in ventral petal lobes. For cells on the dorsal and ventral petal lobes there is significant correlation between cell shape and pollinators. Additionally, sequences of *MIXTA-LIKE* genes were isolated from each of the study species. These genes have been determined to be necessary for formation of conical cells in snapdragon. Understanding the history of cell shape evolution provides a strong foundation for determining the genetic framework for shifts between conical and non-conical cells which may result from changes in the expression and/or function of *MIXTA-LIKE* genes.

INTRODUCTION

Angiosperms contain an enormous amount of diversity, including morphological, ecological and physiological functions (Wikstrom et al., 2001). This diversity has been examined on a macroscopic level, as well as a developmental and structural level, finding major differences across all of the angiosperms (Magallon et al., 1999; Ferrario et al., 2004; Kim et al., 2005; Soltis et al., 2009; Endress, 2011). A critical factor contributing to the success of the angiosperms are the interactions between flowers and the insect pollinators that are attracted to a particular flower (Crepet, 1984). The fitness of insect pollinated flowers relies on the presence and efficiency of its pollinator, which a plant must attract using cues such as visual and/or odor stimuli to which the insect is sensitive, especially in the presence of conspecifics and other species that may be competing for pollinators (Chittka and Raine, 2006). Animal pollinated flowers are often considered to be in one of two major groups, having either generalist pollinators or specialized pollinators. Flowers with specialist pollinators have been seen to have certain adaptations for a specific pollinator or pollinator group, showing a significance of character syndromes (Stebbins, 1970). These syndromes, which have been observed in roughly 75% of flowering plants, are called pollination syndromes, and are defined to include all of the floral traits that are associated with the attraction of a certain group of biotic (animal) or abiotic pollinators (Fenster et al., 2004). Many floral traits have been summarized that place flowers into certain pollination syndromes (Waser, 2006), with many studies showing the selection pressures that certain pollinators place on these floral traits (Bruneau, 1997; Johnson et al., 1998; Fulton and Hodges, 1999; Schemeske and Bradshaw, 1999; Cronk and Ojeda, 2008; Brunet, 2009). Some of these traits, especially flower color, have been debated as to how well they place flowers into certain syndromes or whether they can evolve as a result of alternative selection pressures (Rausher, 2008).

To understand better the interactions between flowers and their pollinators, phylogenetic data are being applied to studies of flowers and pollinators. This allows for inference of the history of the relationship between the flower and pollinators, as well as the ability to detect parallelism and reversals, of which there are many inferred (Armbruster, 1992; Armbruster, 1993; Fenster et al., 2004; Tripp and Manos, 2008; Smith, 2010). Recently, many studies have documented the vast number of times that pollinator transitions have occurred in a given clade (reviewed in Tripp and Manos, 2008), including *Penstemon* (Plantaginaceae) with up to 21 shifts from bee to hummingbird pollination (Wilson et al., 2007), *Cayaponia* (Cucurbitaceae) with multiple repeated shifts from bat to bee pollination (Duchen and Renner, 2010), *Disa* (Orchidaceae) with many transitions occurring to allow up to 19 unique specialized pollination systems (Johnson et al., 1998), and *Costus* (Costaceae) with 7 transitions from bee pollination to hummingbird pollination (Kay et al., 2005).

Many studies go beyond inferring number of pollinator transitions and also investigate traits that are selected upon when subjected to different pollinators including flower orientation, flower color, presence of nectar spurs, landing platforms, nectar guides, and scent (Bruneau, 1997; Johnson et al., 2002; Perez et al., 2006; Goldblatt, 2001; Whittall and Hodges, 2007; Tripp and Manos, 2008; Cronk and Ojeda, 2008; Friedman and Barret, 2008; Lara and Ornelas, 2008; Smith et al., 2008; Schlumpberger et al., 2009; Alcantra and Lohman, 2010; Sletvold et al., 2010, Smith, 2010). Several more studies have gone even further to show that pollination syndromes in sympatric species may maintain species limits (Fulton and Hodges, 1999; Schemeske and Bradshaw, 1999; Kay and Schemeske, 2003). Species delimitations though, may have contributions of factors such as flowering time and not floral traits (Martin et al., 2008).

Of the many traits associated with particular pollination syndromes that have been studied in depth, one trait that is less well characterized, but may contribute to pollination

syndromes, is petal epidermal cell shape. Multiple studies have looked at petal cell shape on a broad, family by family basis, and found that between 60 and 80% of flowers investigated contained conical cells on the petal epidermis (Kay et al., 1981; Christensen and Hansen, 1998). One study looked at petal epidermis cell shape in a single family, Leguminosae, and found that conical cells were prevalent but not always present, usually on the dorsal and lateral petal lobes (Ojeda et al., 2009). Conical cells are considered to be a marker for petal identity (Ronse De Craene, 2008) and have multiple functions. Some of the documented functions of petal conical cells include flower color by light refraction (Noda et al., 1994; Whitney and Glover, 2007), reflectance and transmittance of UV light (Gorton and Vogelmann, 1996), tactile cues for guidance toward nectar reward (Kevan and Lane, 1985), and climate of the flower which may affect nectar, as well as scent of flower (Comba et al., 2010). Conical cells play a major role in bee pollinated flowers, where flowers with flat cells receive fewer pollinators than do those with conical cells (Glover and Martin, 1998). Also, even when bees are attracted to flowers with flat cells, they expend much more energy trying to obtain the nectar reward than would that same bee trying to obtain a reward from a flower with conical cells since the conical cells allow grips for the bee to land on (Whitney et al., 2009).

The developmental framework for conical cells has been worked out in detail for *Antirrhinum majus*, commonly referred to as snapdragon. In snapdragon there are 4 paralogs located in the MYB R2R3 subfamily 9 domain that are responsible for the development of conical cells and trichomes on the petal epidermis. Expression patterns and functional tests of these four genes: *MIXTA*, *MIXTA-LIKE 1*, *MIXTA-LIKE 2*, and *MIXTA-LIKE 3* have determined their role in creating features of the petal epidermis (Noda et al., 1994; Glover et al., 1998; Martin et al., 2002; Perez-Rodriguez et al., 2005; Baumann et al., 2007; Jaffe et al., 2007). Orthologs of these genes have been found to have similar functions in other core eudicots

including *Petunia x hybrida* (Solanaceae; van Houwelingen et al., 1998), *Arabidopsis thaliana* (Brassicaceae; Baumann et al., 2007), and *Gossypium hirsutum* (Malvaceae; Machado et al., 2009), as well as in the early diverging eudicot lineage, *Thalictrum* (Ranunculaceae; di Stilio et al., 2009).

This study focuses on character evolution within the tribe Antirrhineae (Plantaginaceae), to which the model species snapdragon belongs. Here in we test the hypothesis that the evolution of pollinators and petal epidermal cell shape are correlated. Tribe Antirrhineae is an excellent system to address this question because there are three reported transitions from bee pollination to hummingbird pollination within the tribe (Ghebrehiwet et al., 2000). In addition we isolated and identified all copies of *MIXTA-LIKE* genes in the target species, since the *MIXTA-LIKE* genes are responsible for conical cell shape in snapdragon. The initial goal for identifying all copies of *MIXTA-LIKE* genes is to determine if both species with conical cells and those species without conical cells retain all four paralogs of *MIXTA-LIKE* genes.

METHODS

Taxon sampling - A total of 27 taxa were utilized for this study, which are listed in Table

1. The table includes species, seed stocks, GenBank accession numbers for ITS sequences, and accession numbers of vouchers located in the R. L. McGregor Herbarium (KANU), University of Kansas.

Table 1. Table of taxa used in this study. Information includes species name, location seeds were obtained, GenBank accession numbers for ITS, and accession numbers for vouchers placed in the R. L. McGregor Herbarium (KANU). XX-XXXXX for GenBank accession numbers are for sequences that were generated in this study, but not yet deposited in GenBank. Dashes in the seeds and herbarium accession columns indicate that those species were not grown for this study.

Species	Seeds	GenBank	Herbarium
<i>Acanthorrhinum ramosissimum</i>	--	AY731261	--
<i>Albraunia foveopilosa</i>	--	AY731250	--
<i>Annarhinum bellidifolium</i>	Millennium seed bank project	AY731263	JL010
<i>Antirrhinum majus</i>		AY731280	JL004

<i>Asarina procumbens</i>	B & T World Seeds	AF513879	JL006
<i>Chaenorrhinum minus</i>	--	AF513875	--
<i>Cymbalaria muralis</i>	B & T World Seeds	AF513883	--
<i>Galvezia fruticosa</i>	Wayne Elisens, University of Oklahoma	XX-XXXXXX	JL009
<i>Gambelia speciosa</i>	Rancho Santa Ana Botanical Garden	AY731252	JL012
<i>Holzneria spicata</i>	--	AY731258	--
<i>Howelliella ovata</i>	--	AF513899	--
<i>Kickxia elatine</i>	Rancho Santa Ana Botanical Garden	AY731265	JL005
<i>Linaria vulgaris</i>	B & T World Seeds	AF513874	JL015
<i>Lophospermum erubescens</i>	B & T World Seeds	AY731249	JL008
<i>Lophospermum purpusii</i>	B & T World Seeds	XX-XXXXXX	JL007
<i>Mabrya acerifolia</i>	Wayne Elisens, University of Oklahoma	XX-XXXXXX	--
<i>Mabrya rosei</i>	Wayne Elisens, University of Oklahoma	XX-XXXXXX	JL014
<i>Maurandella antirrhiniflora</i>	B & T World Seeds	AF513878	JL013
<i>Maurandya scandens</i>	B & T World Seeds	XX-XXXXXX	JL003
<i>Misopates orontium</i>	Millennium seed bank project	AY731260	JL011
<i>Mohavea confertiflora</i>	--	AF513891	--
<i>Neogaerrhinum strictum</i>	--	AF513904	--
<i>Pseudomisopates rivas mertinezii</i>	--	AY731262	--
<i>Pseudorontium cyathiferum</i>	--	AF513884	--
<i>Rhodochiton atosanguineum</i>	B & T World Seeds	XX-XXXXXX	JL001
<i>Sairocarpus coulterianum</i>	Rancho Santa Ana Botanical Garden	AY878117	--
<i>Schweinfurthia pedicellata</i>	--	AY731256	--

Phylogenetic analysis - Sequences of Internal Transcriber Spacer (ITS) 1 and 2 from Vargas et al. (2004) were downloaded from GenBank. Additional sequences for *Galvezia fruticosa*, *Lophospermum purpusii*, *Mabrya acerifolia*, *M. rosei*, *Maurandya scandens*, and *Rhodochiton atosanguineum* were added to analysis using the same primers (ITS 1 and 4) as in Vargas et al. (2004). DNA was extracted from these additional taxa using Promega Wizard kit (Promega, Madison, Wisconsin, USA) and then treated with RNase. PCR conditions using ITS

primers 1 and 4 contained 2 μ L of DNA, 5X PCR buffer, 2mM MgCl₂, 0.5 μ M of each primer, 0.8 mM dNTPs, and 1.25 unit of GoTaq (Promega, Madison, Wisconsin, USA). Sequencing was carried out on ExoSap cleaned PCR products and sequenced in both forward and reverse directions. Sequences were aligned using MUSCLE (Edgar, 2004), followed by manual adjustment in MacClade v4.08 (Maddison and Maddison, 2005). Nucleotide sequence alignments were used to generate estimates of the species phylogeny under Maximum Parsimony (MP), Maximum Likelihood (ML) and Bayesian criteria. Maximum likelihood was implemented in Garli (Zwickl, 2006) using the GTR + I + Γ model of molecular evolution as specified by jModeltest (Posada, 2008). Support values were generated using MP in Paup* 4.0 (Swofford, 2002) with 1000 heuristic bootstrap replicates and the TBR branch swapping algorithm. Support values were also generated using ML with 1000 bootstrap replicates in Garli as described above. Bayesian criterion was implemented using MrBayes (Huelsenbeck and Ronquist, 2001; Ronquist and Huelsenbeck, 2003) and the GTR + I + Γ model of molecular evolution with two Markov chains running for 1,000,000 generations sampling every 1,000th generation. At completion of runs, the two chains were checked for convergence and the first 25% of saved trees were discarded as initial burn-in. Remaining trees were used to calculate posterior probabilities of node support in a 50% majority-rule consensus tree.

Pollinators - Using the maximum likelihood tree, we traced pollinators on to the tree using parsimony criteria in MacClade v4.08 (Maddison and Maddison, 2005). Pollinators were coded as binary characters. According to Ghebrehiwet et al. (2000), we expected to see three independent shifts. Anomalies for coding of pollination system occurred in the genus *Lophospermum*. *Lophospermum erubescens* is reported to be hummingbird pollinated (Elisens, 1986), where as *L. purpusii* has an unknown pollinator (Elisens and Freeman, 1988). However, the phenotype of these two species appears to fit better with a bee pollination syndrome, rather

than a hummingbird pollinated syndrome. The flowers are pink in color, with a wide corolla tube, horizontal orientation and presence of nectar guides. Table 2 shows the inferred pollinator for each species, as well as the reference for this inference.

Table 2 Species included in this study, with inferred pollinators from the literature with appropriate references.

Species	Inferred pollinator	Reference
<i>Acanthorrhinum ramosissimum</i>	bee	Sutton, 1988
<i>Albraunia foveopilosa</i>	bee	Sutton, 1988
<i>Annarhinum bellidifolium</i>	bee	Sutton, 1988
<i>Antirrhinum majus</i>	bee	Sutton, 1988
<i>Asarina procumbens</i>	bee	Sutton, 1988
<i>Chaenorrhinum minus</i>	bee	Sutton, 1988
<i>Cymbalaria muralis</i>	bee	Sutton, 1988
<i>Galvezia fruticosa</i>	hummingbird	Elisens, 1986; Elisens, 1992
<i>Gambelia speciosa</i>	hummingbird	Elisens, 1986
<i>Holzneria spicata</i>	bee	Sutton, 1988
<i>Howelliella ovata</i>	bee	Thompson, 1988
<i>Kickxia elatine</i>	bee	Sutton, 1988
<i>Linaria vulgaris</i>	bee	Sutton, 1988
<i>Lophospermum erubescens</i>	hummingbird	Elisens, 1986
<i>Lophospermum purpusii</i>	unknown	Elisens & Freeman, 1988
<i>Mabrya acerifolia</i>	hummingbird	Elisens & Crawford, 1988
<i>Mabrya rosei</i>	hummingbird	Elisens, 1986
<i>Maurandella antirrhiniflora</i>	bee	Elisens, 1986
<i>Maurandya scandens</i>	bee	Elisens, 1986
<i>Misopates orontium</i>	bee	Sutton, 1988
<i>Mohavea confertiflora</i>	bee	Little, 1983
<i>Neogaerrhinum strictum</i>	bee	Sutton, 1988
<i>Pseudomisopates rivas mertinezii</i>	bee	Sutton, 1988
<i>Pseudorontium cyathiferum</i>	bee	Elisens, 1986; Elisens & Freeman, 1988
<i>Rhodochiton atrosanguineum</i>	hummingbird	Elisens, 1986
<i>Sairocarpus coulterianum</i>	bee	Elisens & Freeman, 1988
<i>Schweinfurthia pedicellata</i>	bee	Sutton, 1988

Cell shape - Shape of cells on the adaxial (inner) epidermal surface of petals was measured by sectioning petals from both the dorsal (adaxial) and ventral (abaxial) sides of flowers. Fresh petal material was fixed using glutaraldehyde (5% glutaraldehyde solution in 0.1 M phosphate buffer) overnight and then dehydrated through an ethanol series. Tissue was then wax embedded as described in Jackson (1991) and Preston and Kellogg (2007). Sections were

then stained with Toulidine blue and slide images were documented using a Leica DM5000B microscope attached to a Leica DFC300FX camera. Images were then imported in ImageJ where height and width at half height were taken for 18 to 30 cells for each species. The ratios of these numbers were then taken to arbitrarily separate conical from non-conical cells. Species with an average ratio over 0.9 were classified as conical, where as non-conical cells had a ratio of 0.9 or lower. SEM images were taken of the petal epidermis to give corroboration with the wax sectioning. Mature flowers of tested species were fixed in glutaraldehyde (5% glutaraldehyde solution in 0.1 M phosphate buffer) overnight and then dehydrated through an ethanol series. Dehydrated flowers were critical point dried using a Tousimis critical point dryer and then dissected into sepals, base of petal tube, and petal lobe. Tissue was collected for imaging the adaxial surface of dorsal petals. Specimens were mounted on stubs, sputter-coated with gold, and viewed with a D. Leo field emission scanning electron microscope.

Once cell shape was determined for target species, the trait was mapped on to the maximum likelihood tree to determine number of transitions. First, cell shape was coded as a binary character, with 0 being conical (ratio above 0.9) and 1 for non-conical (ratio under 0.9). This trait was then traced on to the maximum likelihood tree using MacClade v4.08 (Maddison and Maddison, 2005).

Correlation test - Using the Discrete function in BayesTraits we tested for correlation between petal epidermal cell shape (conical vs. non-conical) and pollination system (bee vs. bird pollinated flowers) using the maximum likelihood tree with branch lengths representing time, as well as the binary coded traits pollinator type and cell shape. After coding pollinator type as 0 for bee pollinated and 1 for hummingbird pollinated, and cell shape as 0 for conical and 1 for non-conical we were able to test two separate models of trait evolution on the data. The first model allowed the two parameters, pollinator type and cell shape, to vary independently from

each other, and the second model restricted pollinator type and cell shape to vary dependently. Both models were conducted with 1000 optimization attempts. A log likelihood ratio test was then conducted using a chi-square distribution with degrees of freedom of 4.

Isolation of MIXTA-LIKE genes - Total RNA was isolated from three stages of development from target species' flowers using Trizol following the manufacturer instructions (Ambion, Austin, Texas, USA) and DNase treated using TurboDNA (Ambion, Austin, Texas, USA). cDNA was generated using 1 µg of total RNA in a 15 µl cDNA synthesis reaction using iScript Synthesis Kit following the manufacturer instructions (BioRad, Hercules, California, USA). Orthologs of *MIXTA*, *MIXTA-LIKE 1*, *MIXTA-LIKE 2*, and *MIXTA-LIKE 3* were isolated from floral cDNA by reverse-transcriptase PCR (RT-PCR) using a degenerative forward and reverse primer to amplify roughly 350 bases of conserved region of each gene. *MIXTA* genes were isolated using forward primer (5'-GTGAAAAAAGGGCCATGGAC-3') and reverse primer (5'-CCCAGGATGTTATGAKTST-3'). *MIXTA-LIKE 1* was amplified using forward primer (5'-CCATGGACACCCWGAMGAAG-3') and reverse primer (5'-GYTGGCCACAACCWAGGAC-3'). *MIXTA-LIKE 2* was amplified using forward primer (5'-CTGAAGAAGATCAGAAGC-3') and reverse primer (5'-GCCATGTGGCTSAGATTKC-3'). *MIXTA-LIKE 3* was amplified using forward primer (5'-CTGAAGAAGACCARAAGC-3') and reverse primer (5'-TGCCGAGCGCTCTCCCA-3'). RT-PCR reactions contained 2 ul of 1:10 diluted cDNA, 1.25 units GoTaq (Promega, Madison, Wisconsin, USA), 5X PCR buffer, 2mM MgCl₂, 0.5 µM of each primer, and 0.8 mM dNTPs. PCR reactions were run for 40 cycles with a gradient annealing temperature of 47°C - 60°C. PCR products were subjected to gel electrophoresis using a 1.5% agarose gel and samples with appropriate sized product were gel-purified using the Wizard SV Gel and PCR Clean Up System Kit (Promega, Madison, Wisconsin, USA) before being cloned. Gel-purified PCR products were cloned into the pGEM -T vector system

(Promega, Madison, Wisconsin, USA) following the manufacturer instructions. Eight clones were sequenced using M13 forward and M13 reverse primers in order to identify multiple gene copies amplified by our RT-PCR approach (Howarth and Baum, 2005).

Sequences of *MIXTA-LIKE* genes were imported to MacClade v4.08 (Maddison and Maddison, 2005) and aligned by eye. Maximum likelihood analysis was implemented in Garli (Zwickl, 2006) using the GTR + I + Γ model of molecular evolution to determine the maximum likelihood tree. Maximum likelihood bootstrap support with 500 replicates, and bayesian posterior probability with 5,000,000 generations sampled every 1000 was conducted as described above to assess orthology of gene sequences. GenBank accession numbers of *MIXTA-LIKE* genes used can be found in Appendix 2.

RESULTS

Phylogenetic analysis - The phylogeny generated in this study using ITS sequences closely matches that of Vargas et al. (2004). Figure 6 shows the maximum likelihood tree, with bootstrap support values of recovered clades shown. High support values appear for the major clades of the tribe. The clade containing *Gambelia* has bootstrap support values of 100% (MP) and 99% (ML) as well as a posterior probability of 1.0. The *Maurandya* clade containing *Asarina*, *Cymbalaria*, *Lophospermum*, *Mabrya*, *Maurandya*, and *Rhodochiton* is also well supported with bootstrap values of 91% (MP) and 100% (ML) and a posterior probability of 1.0. The clade containing the *Galvezia* genus has support values of 98% (MP) and 96% (ML) and a posterior probability of 1.0. Even though some of the species level relationships are not well resolved, having the major clades with high support values provides more confidence in pollinator transitions.

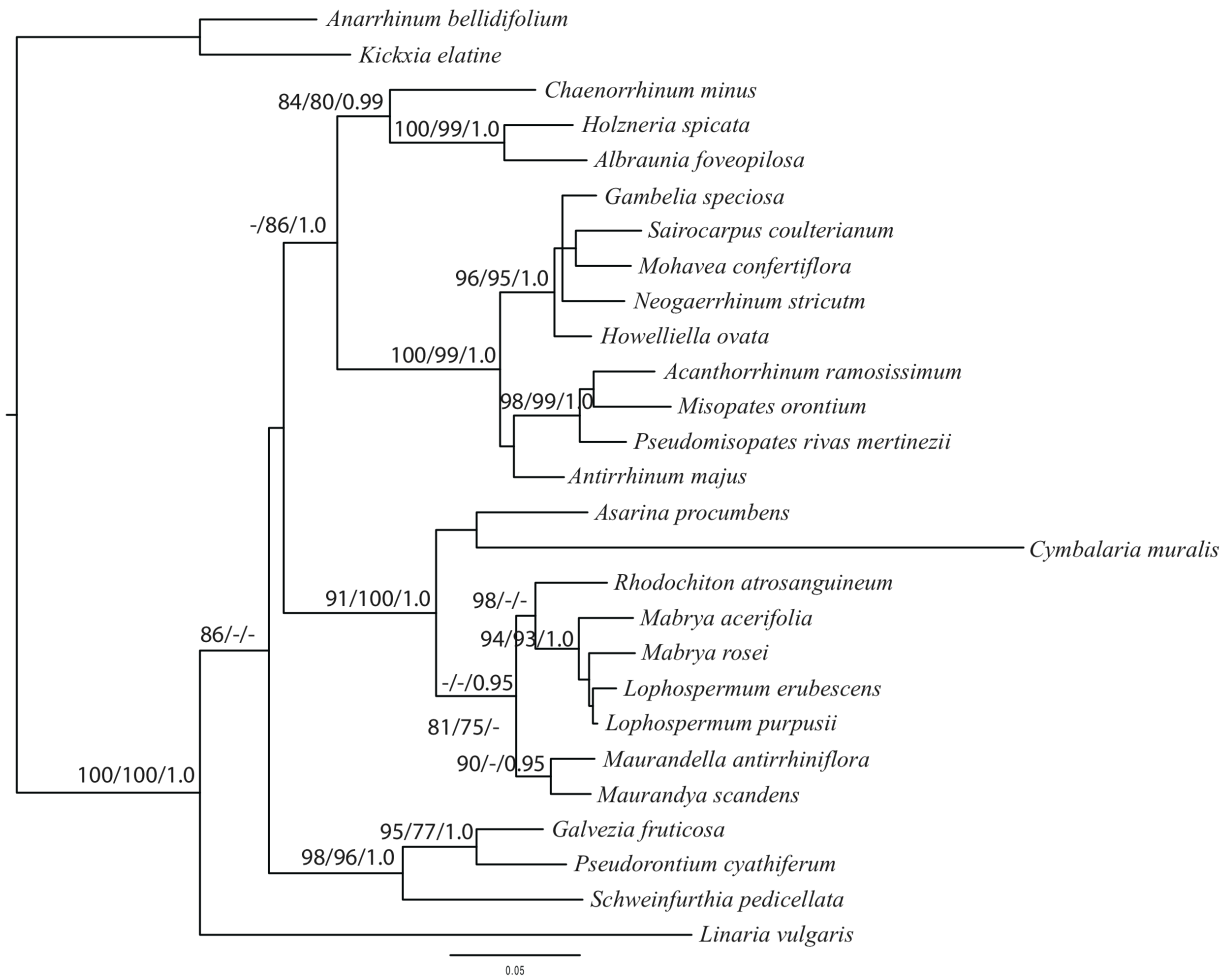


Figure 6. Phylogeny of ITS with sequences downloaded from GenBank (Vargas et al. 2004) and augmented with additional sequences using ITS primers 1 and 4. Shown is maximum likelihood tree, with support values from bootstrap replicates of MP/ML/BI.

Tracing character history: pollinator type and cell shape - Tracing pollinator types using MP onto the maximum likelihood tree revealed three independent transitions from the ancestral state of bee pollination to a derived state of hummingbird pollination (Fig. 7). These three transitions occur in the *Maurandya* clade, with *R. atrosanguineum*, *M. rosei*, *M. acerifolia*, and *L. erubescens*, reported to be hummingbird pollinated (Elisens, 1986; Elisens & Crawford, 1988; Elisens & Freeman, 1988), as well as in *Gambelia* and *Galvezia* both of which are reported to be hummingbird pollinated (Elisens, 1986; Elisens, 1992) (Table 2). There also appears to be a possible reversal to bee pollination within *Lophospermum*. Ghebriwet et al. (2000) also inferred three independent transitions from bee to hummingbird pollination, though their

transitions differ from ours. In their study, the three transitions to hummingbird pollination occur within *Rhodochiton*, a clade containing *Gambelia* and *Galvezia*, and the *Howelliella* which was reported to be both bee and hummingbird pollinated. In the present study, *Gambelia* and *Galvezia* are not resolved as a monophyletic lineage, and *Howelliella* is coded as a bee pollinated species.

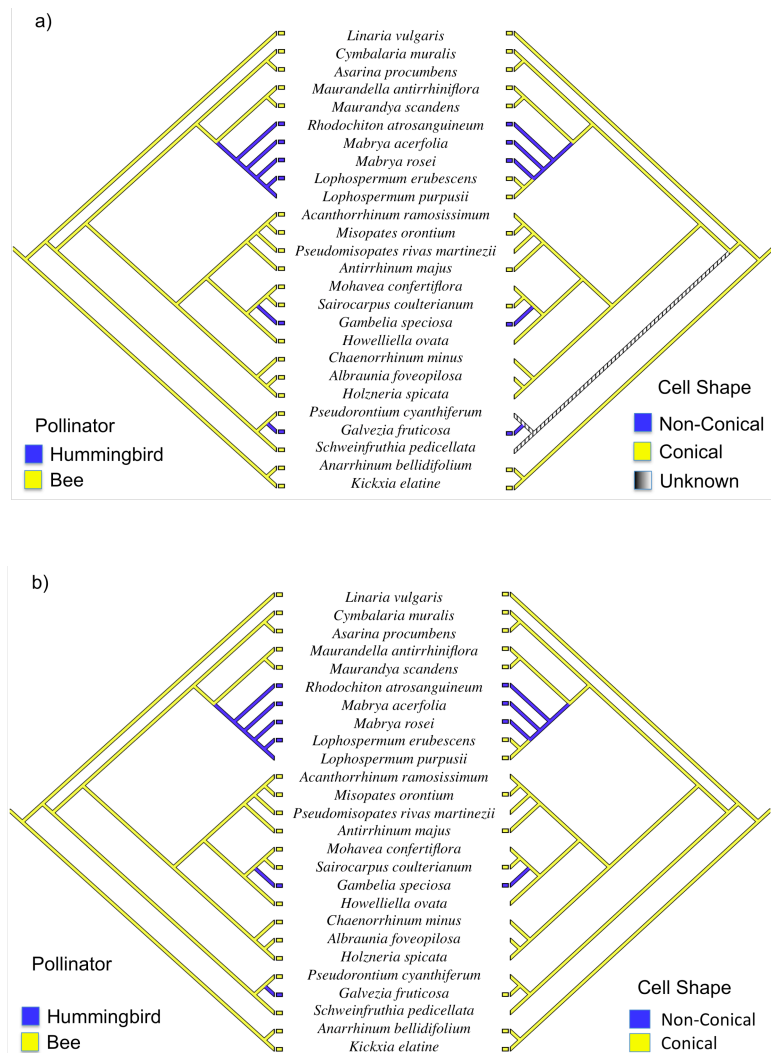
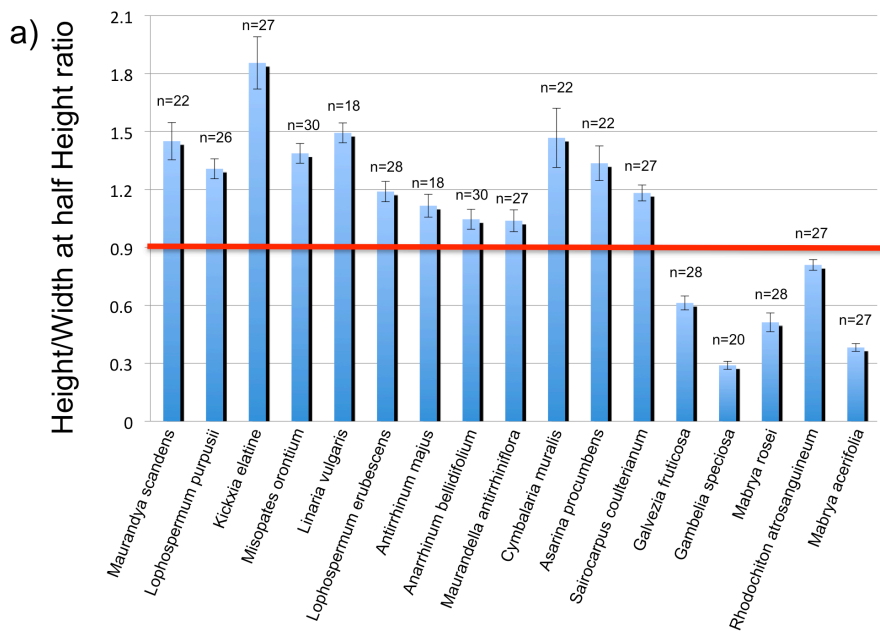


Figure 7. MP reconstruction of pollinator system and cell shape on to the ML phylogeny. a) pollinator system and cell shape on dorsal petal lobes. Three independent shifts appear from bee pollination to hummingbird pollination (left side) with three corresponding shifts from conical to non-conical cells (right side). b) same mapping except for ventral petal lobe cells. Again there are three shifts from bee pollination to hummingbird pollination, but this time only two transitions from conical to non-conical.

After measuring cell shape for the dorsal and ventral petals of 17 species we were able to separate species into either having conical or non-conical cells (Fig. 8). Cells with a height/width at half height ratio greater than 0.9 were classified as conical, and cells with a ratio

of less than 0.9 were classified as non-conical. Figure 9 shows examples of both classifications of cell shape. Five of 17 species had non-conical cells on the dorsal petal epidermal surface, with the other 12 species exhibiting conical cells on dorsal petals (Fig. 8). Species possessing non-conical cells include *G. fruticosa*, *G. speciosa*, *M. acerifolia*, *M. rosei*, and *R. atrosanguineum*. Cell shape on the ventral petal lobes showed a slightly different pattern. Four of 17 species exhibited non-conical cells and the remaining 13 species had conical cells on ventral petal lobes. The non-conical species for the ventral petal lobe cells include *G. speciosa*, *M. acerifolia*, *M. rosei*, and *R. atrosanguineum*. Transitions in cell shape for the dorsal and ventral petal lobes were traced separately on to the maximum likelihood tree using parsimony. Figure 7a shows that for dorsal petals there appear three independent transitions from conical cells to non-conical cells, with one reversal from non-conical cells to conical cells. Figure 7b shows a similar pattern for transitions in cell shape on the ventral petal lobe, but with only two independent transitions from conical to non-conical cells, and one reversal to conical cell shape.



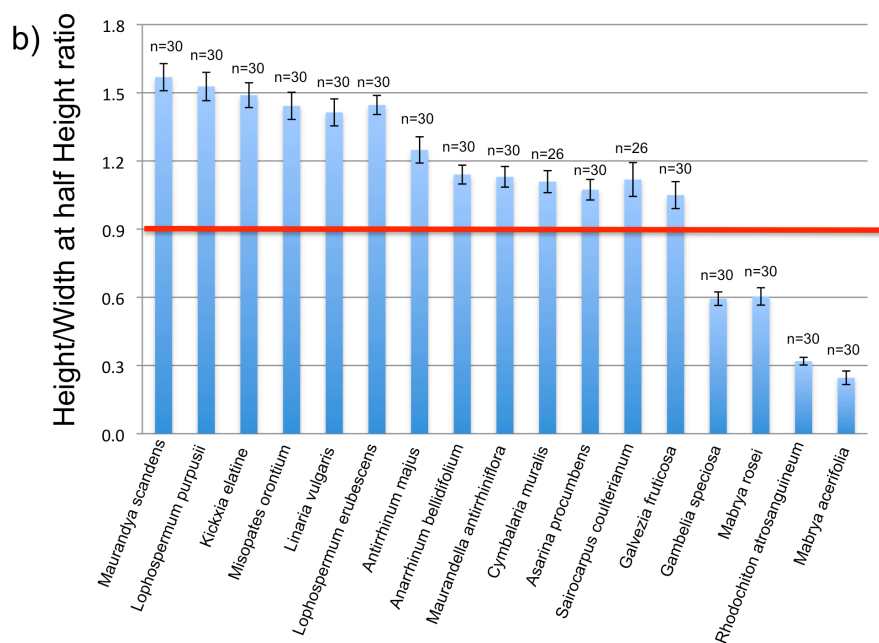
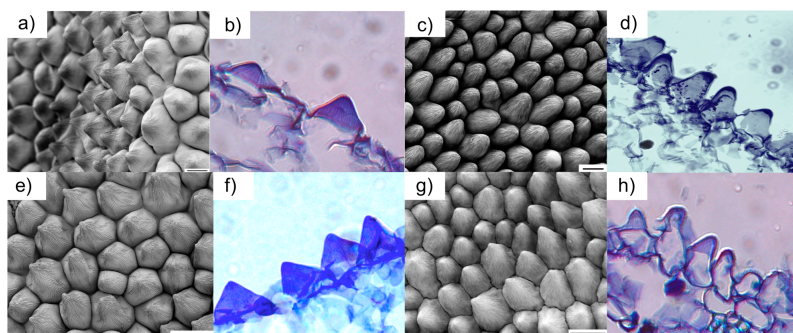


Figure 8. Height/width ratios of petal epidermal cells from a) dorsal petal lobes and b) ventral petal lobes. The red line is the cut off between conical and non-conical cells, with a ratio of 0.9. For the dorsal petal lobes (a), there are five species that possess non-conical cells, while for the ventral petal lobes (b) there are four species that possess non-conical cells. Above each bar is the number of cells measured.

Conical cells



Non-conical cells

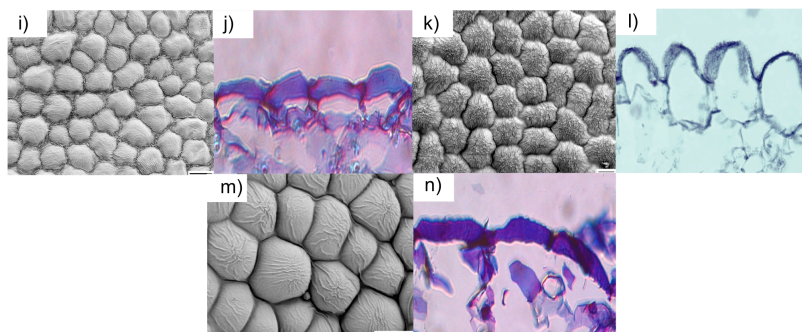


Figure 9. Visual representation of conical and non-conical cells. Each example consists of SEM images and wax sections of cells to give a good representation of each. a & b) *Antirrhinum majus* dorsal petal lobes, c & d) *Lophospermum purpusii* dorsal petal lobes, e & f) *Misopates orontium* dorsal petal lobes, g & h) *Kickxia elatine*

dorsal petal lobes, i & j) *Mabrya acerifolia* dorsal petal lobes, *Rhodochiton atrosanguineum* dorsal petal lobes, and m & n) *Galvezia fruticosa* dorsal petal lobes. Scale bars on the SEM images correspond to 20 μm .

Correlation analysis - The correlation analysis was conducted running two models in a likelihood framework. The first model allowed both traits, cell shape and pollinator type to vary independently of each other. The second model constrained the two traits to depend on each other while evolving across our input phylogeny. Comparing these two models for data on pollinators and cell shape from dorsal petals gave a likelihood ratio test statistic of 13.39, which when compared to a chi-square distribution with four degrees of freedom, resulted in a p-value of 0.0095. Analysis of data on pollinators and cell shape from ventral petals yielded a likelihood ratio test statistic of 9.49, p-value of 0.0499. Results from our correlation analyses indicate that both dorsal and ventral cells show a significant correlation of cell shape with pollinator type. The dependent models for each test calculated transition rates for each combination of traits. Although transition rates varied from zero to 526.5, for data from both dorsal petal lobe and ventral petal lobe cells, the highest estimated transition rate was from bee pollinated flowers with non-conical cells to hummingbird pollinated flowers with non-conical cells (Fig 10).

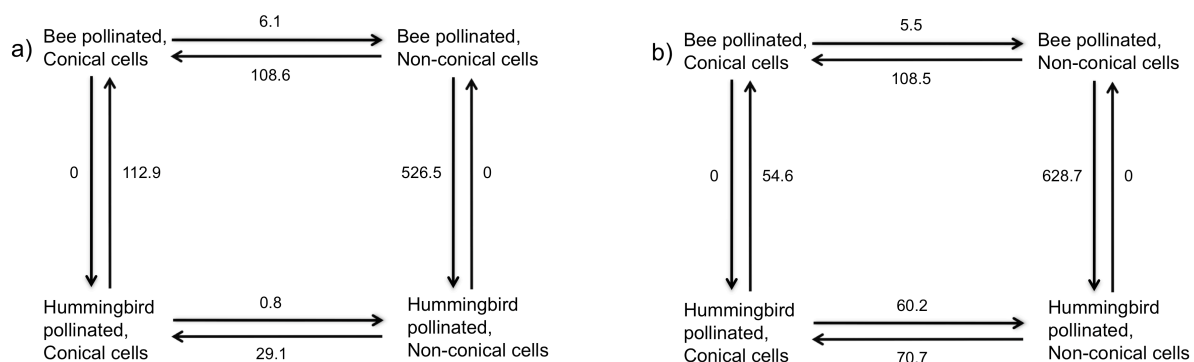


Figure 10. Reported transitions from the dependent model in the correlation analysis. a) represents cells on the dorsal petal lobe and b) represents cells on the ventral petal lobes. For both cases the highest transition rate was from a bee pollinated flower with non-conical cells to a hummingbird pollinated flower with non-conical cells.

Isolation of MIXTA-LIKE genes - Partial sequences from four orthologs of *MIXTA-LIKE* genes were isolated and identified from each of the 17 species investigated in this study, shown in Fig. 11. Copies of *MIXTA-LIKE 2* from *Kickxia elatine* and *Misopates orontium*, as well as *MIXTA-LIKE 1* from *Anarrhinum bellidifolium*, could not be amplified. Gene sequences range in size from 331 to 390 bp, with *MIXTA* and *MIXTA-LIKE 1* having 331 bp, *MIXTA-LIKE 2* with 358 bp, and *MIXTA-LIKE 3* with 390 bp. Phylogenetic analysis of the gene sequences yield two distinct clades, *MIXTA/MIXTA-LIKE 1* and *MIXTA-LIKE 2/MIXTA-LIKE 3*. These clades have support values of 100/1.0. Within these two larger clades, the *MIXTA/MIXTA-LIKE 1* clade is separated into two unique clades, each containing one ortholog from each sampled species. Support values for these clades are 91/1.0 and 75/1.0 respectively. The clade consisting of *MIXTA-LIKE 2/MIXTA-LIKE 3* does not form two unique clades, with some orthologs grouping with different genes from closely related species, than with other orthologs of the same gene. Support values within this clade are weak.

DISCUSSION

The evolution of petal cell shape is correlated with pollinators - This study was designed to test for a correlation between pollinator types and petal epidermal cell shape. Two studies have suggested that 60-80% of all angiosperms have conical cells on the petal epidermis (Kay et al., 1981; Christensen and Hansen, 1998); a recent study investigating a single family showed similar results (Ojeda et al., 2009). Using a phylogeny with well-resolved, highly supported clades for tribe Anitrrhineae (Fig. 6), we identified three independent transitions from bee pollination to hummingbird pollination, and similar transitions from conical to non-conical petal epidermal cell shape (Fig. 7). Additional analyses showed a significant correlation between pollinator type and cell shape for both dorsal and ventral petal lobes. This correlation is noteworthy because this the first time that presence or absence of conical cells has been

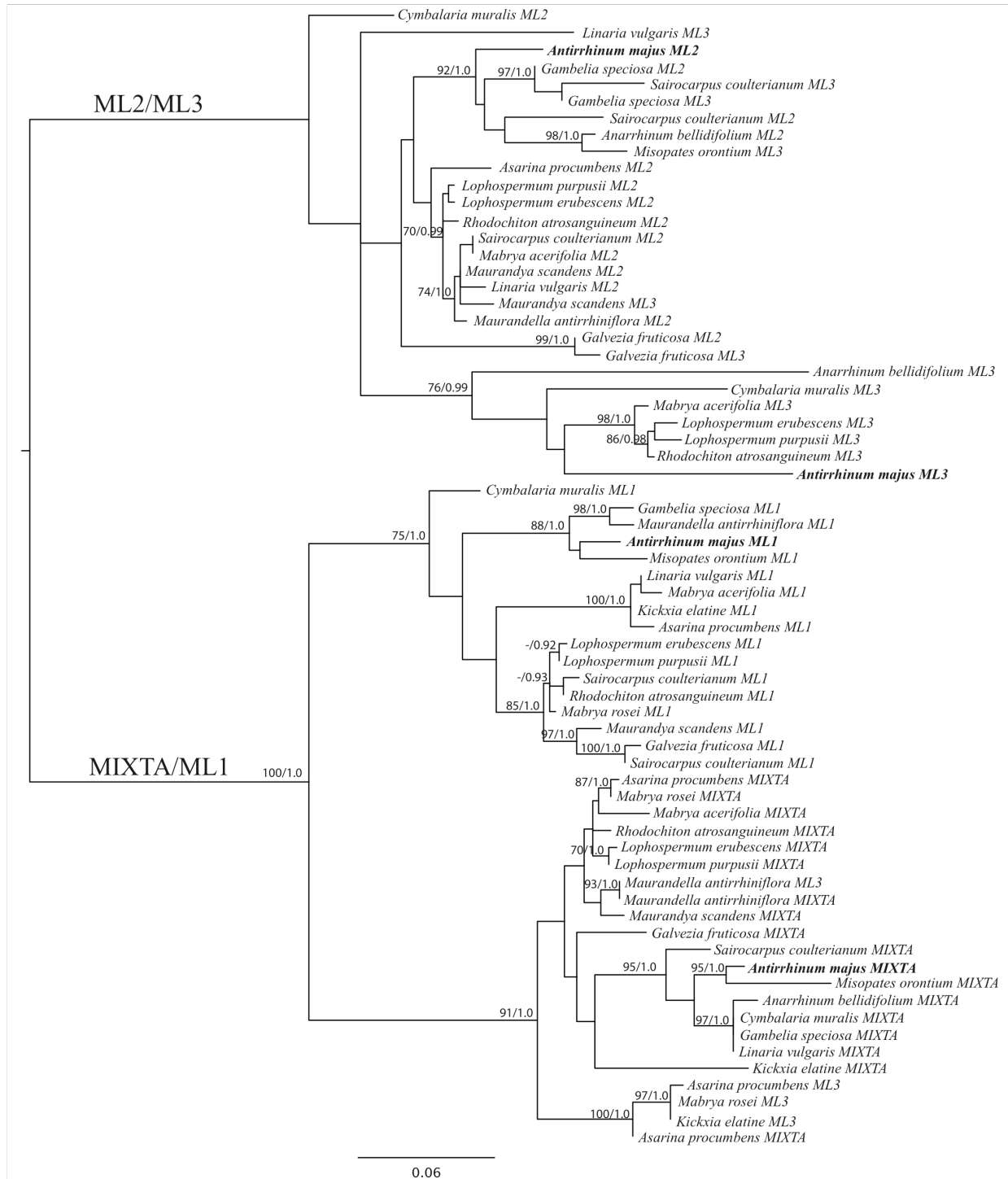


Figure 11. Gene tree containing the four orthologs of *MIXTA-LIKE* genes isolated from target species. Shown is the ML tree, with support values of ML bootstrap and Bayesian posterior probability. There is high support for two distinct clades that constitute mainly *MIXTA/MIXTA-LIKE 1* and *MIXTA-LIKE 2/MIXTA-LIKE 3*. Fairly strong support for two clades each containing primarily *MIXTA* and *MIXTA-LIKE 1*. No such support for individual clades of *MIXTA-LIKE 2* and *MIXTA-LIKE 3* exists. Bootstrap support values less than 70 are not shown. *MIXTA-LIKE* genes from snapdragon are bolded for reference.

associated with pollination system. Christensen and Hansen (1998) speculated on a large scale that presence of conical cells is primarily associated with bee pollination, where as loss of conical cells may be associated with bird pollination. However, that study investigated many families from across angiosperm diversity and failed to account for phylogenetic history. This study gives strong support to the assertion that there is an association between pollination system and petal epidermal cell shape.

Most studies that investigate pollinator mediated selection measure floral traits from one species along with female or male fitness to determine if particular traits confer a significant fitness improvement, primarily through pollinator attraction and pollinator efficiency (Sletvold et al., 2010). Examples include longer flower tubes in *Gladiolus* (Alexandersson and Johnson, 2002), wider corollas in *Ipomopsis* (Campbell et al., 1996), experimental flower color in snapdragons (Jones and Reithel, 2001), larger petals and altered flowering in *Arabidopsis* (Sandring and Agren, 2009), and nectar reward and larger displays in *Iochroma* (Smith et al., 2009). Additionally, many intraspecific studies investigate multiple selective traits, since by definition pollination syndromes are suites of traits that affect pollination, presuming that a single trait may not be affected at all or as expected by the pressures of pollinators (Castelanos et al., 2004; Fenster et al., 2004; Dudash et al., 2011). Finally, there is evidence that intraspecific variation in floral form, such as seen in *Gorteria*, can arise in the absence of pollinator shifts (Ellis and Johnson, 2009). In addition to intraspecific approaches, which provide evidence for the adaptive significance of floral traits, macroevolutionary studies using phylogeny-based comparative methods that identify correlated trait evolution provide evidence for adaptation (Harvey and Pagel, 1991). The significant correlation found in this study between petal epidermal cell shape and pollinators can be added to the many comparative-method based studies that have found evidence that pollinators exert selective pressures on floral traits (Bruneau, 1997;

Johnson et al., 2002; Perez et al., 2006; Whittall and Hodges, 2007; Tripp and Manos, 2008; Friedman and Barret, 2008; Smith et al., 2008; Alcantra and Lohman, 2010; Smith, 2010).

A high rate of transition to hummingbird pollinators in the context of non-conical cells

Given that there is significant correlation between changes in petal epidermal cell shape and pollinators, one might expect that the highest rate of evolutionary transition in this system would be from hummingbird pollination with conical cells to hummingbird pollination with non-conical cells – essentially that evolutionary loss of conical cells occurs by genetic drift after transitions to hummingbird pollination. This hypothesis is consistent with evidence suggesting that conical cells are important for both attracting bees and increasing efficiency during bee visitation (Glover and Martin, 1998; Noda et al., 1994; Whitney and Glover, 2007; Whitney et al., 2009), and a lack of evidence implicating non-conical cells in the attraction and/or pollination efficiency of hummingbirds. For data from both the dorsal and ventral petal lobes, the transition rate from hummingbird/conical cells to hummingbird/non-conical cells was quite low (Fig. 10). Instead, for data on epidermal cell shape from both dorsal and ventral petal lobes, the character state transition with the highest associated rate was from bee pollinated flowers with non-conical cells to hummingbird pollinated flowers with non-conical cells (Fig. 10). These data suggest that shifts to hummingbird pollination are facilitated in a background of non-conical petal epidermal cells. This result is inconsistent with the hypothesis that conical cells are lost by drift when selection pressures to maintain them in the context of bee pollination are relaxed. However, this result may be consistent with views that flowers undergo adaptive evolution of traits that discourage certain pollinators instead of attracting others during the evolution of pollinator switching (Castelanos et al., 2004). During a transition period, when flowers might be capable of pollination by both bees and hummingbirds (a polymorphic state not represented in our analyses), transitions to complete hummingbird pollination may be facilitated by the presence of

non-conical cells, not because non-conical cells facilitate hummingbird pollination, per se, but because non-conical cells discourage bee visitation.

The theory that loss of conical cells evolved to discourage bee pollination during transition from bee to hummingbird pollination adds to a growing body of evidence where selection of certain floral traits discourages a group of pollinators. Other examples include floral color with two explicit examples. The first is the role that flower color plays between *Mimulus cardinalis* and *M. lewisii* (Phrymaceae). These two species can be found in sympatry, but remain distinct species predominately by the red flowers of *M. cardinalis* discriminating against the bees that pollinate the pink *M. lewisii* (Schemeske and Bradshaw, 1999; Bradshaw and Schemeske, 2003). A second example of flower color is in *Petunia* where altered pink flowers are less attractive to their normal hawkmoth pollinators than wildtype white flowers (Hoballah et al., 2007). Other floral traits that discourage pollinators can be found in *Penstemon* where stigma exsertion, corolla constriction, and pendent flowers discourage bee pollination (Castelanos et al., 2004). Corolla constriction has also been documented in discouraging bee pollinators in Polemoniaceae (Grant and Grant, 1965). Pollen presentation patterns have been documented to discourage pollinators based on the presence or absence of what are termed good and bad pollinators (Thomson and Thomson, 2002). Another trait that can deter certain pollinators is the scent of the flower determined by the release of volatiles that are found to be unpleasant to some pollinators (Schiestl et al., 2011). Petal epidermal cell shape may fit into this list of floral traits that evolved to discourage one type of pollinator, instead of attracting a different pollinator type.

Loss of conical cells can be variable across the flower - For the vast majority of the species examined in this study, petal epidermal cell shape is relatively consistent across all of the petal lobes of the flower. In most species, if the dorsal petal lobe cells are non-conical, then the ventral petal lobe cells are also non-conical (Figs. 8a & 8b). Even though the ratios of

height/width are not exactly the same for both petal lobes, the ratios usually differ by less than 0.3, and stay in the same categories of conical or non-conical (Fig. 8). However, one species, *Galvezia fruticosa* differs from this usual pattern. Cells of the dorsal petal lobes of *G. fruticosa* are determined to be non-conical (ratio of 0.6), whereas on the ventral petal lobe cells are conical (ratio of 1.0). This is suggestive that unique changes in developmental pathways may be responsible.

Evidence suggests that *G. fruticosa* conical cell formation is not controlled identically across the dorsal and ventral regions of the flower. Differing development pathways involving conical cell formation within a single flower has been previously documented (Noda et al., 1994). An ortholog of *MIXTA-LIKE 2*, termed *PhMYB1*, has been isolated from *Petunia x hybrida*. Mutants of *phmyb1* show loss of conical cells, similar to snapdragon *mixta* mutants (Baumann et al., 2007). However, *phmyb1* mutants develop non-conical, relatively flat cells on the outer (abaxial) petal epidermis, whereas the inner (adaxial) petal epidermis is comprised of conical cells (Baumann et al., 2007). This work demonstrates that the cellular developmental control of conical cell formation does not have to be identical throughout the flower.

A role for MIXTA genes cell shape evolution - Pioneering studies in snapdragon have determined the necessity of four orthologs *MIXTA*, *MIXTA-LIKE 1*, *MIXTA-LIKE 2* and *MIXTA-LIKE 3* for conical cell formation (Noda et al., 1994; Glover et al., 1998; Martin et al., 2002; Perez-Rodriguez et al., 2005; Baumann et al., 2007; Jaffe et al., 2007). Orthologs of these genes have been found to have similar functions in other core eudicots including *Petunia x hybrida* (van Houwelingen et al., 1998), *Arabidopsis thaliana* (Baumann et al., 2007), and *Gossypium hirsutum* (cotton, Machado et al., 2009), as well as in the early diverging eudicot lineage, *Thalictrum* (di Stilio et al., 2009). These studies make the *MIXTA-LIKE* genes strong candidates for determining the developmental genetic basis for shifts in cell shape seen in this study.

In addition to finding a significant correlation between pollinator types and petal epidermal cell shape, partial sequence of the four *MIXTA-LIKE* orthologs were identified from most species in this study. With the exception of *MIXTA-LIKE 2* in *Kickxia elatine* and *Misopates orontium*, and *MIXTA-LIKE 1* in *Anarrhinum bellidifolium*, all four orthologs have been identified from all study species. Additional data are required to determine if lack of isolation of these paralogs is due to gene divergence or genes loss. Finding all four *MIXTA-LIKE* paralogs from the Antirrhineae taxa sampled, suggests that three duplication events, giving rise to four *MIXTA-LIKE* paralogous lineages, occurred before the diversification of Antirrhineae. The implications for the presence of all four paralogs in each species is that if the *MIXTA-LIKE* genes are contributing to loss of conical cells, it is not by gene loss (*K. elatine*, *M. orontium* and *A. bellidifolium* all have conical petal epidermal cells). Rather, these genes may have altered expression patterns or functions. A future direction of this project is to investigate the expression patterns of each paralog in a given species, and across transitions in pollination type and loss of conical cells.

REFERENCES

- Alcantara, S. and L. G. Lohmann. 2010. Evolution of floral morphology and pollination system in Bignoniaceae (Bignoniaceae). *American Journal of Botany* 97: 782-796.
- Alexandersson, R. and S. D. Johnson. 2002. Pollinator-mediated selection on flower-tube length in a hawkmoth-pollinated *Gladiolus* (Iridaceae). *Proceedings: Biological Sciences* 269: 631-636.
- Ambrose, B. A., D. R. Lerner, P. Ciceri, C. M. Padilla, M. F. Yanofsky and R. J. Schmidt. 2000. Molecular and genetic analyses of the *Silky1* gene reveal conservation in floral organ specification between eudicots and monocots. *Molecular Cell* 5: 569-579.
- Armbruster, W. S. 1992. Phylogeny and the evolution of plant-animal interactions. *BioScience* 42: 12-20.
- Armbruster, W. S. 1993. Evolution of plant pollination systems: hypotheses and tests with neotropical Vine, *Dalechampia*. *Evolution* 47: 1480-1505.
- Baumann, K., M. Perez-Rodriguez, D. Bradley et al. 2007. Control of cell and petal morphogenesis by R2R3 MYB transcription factors. *Development* 134: 1691-1701.
- Borchert, T., K. Eckardt, J. Fuchs, K. Kruger and A. Hohe. 2009. 'Who's who' in two different flower types of *Calluna vulgaris* (Ericaceae): morphological and molecular analyses of flower organ identity. *BMC Plant Biology*, 9.
- Bowman, J. L. 1997. Evolutionary conservation of angiosperm flower development at the molecular and genetic levels. *Journal of Bioscience* 22, 515-527.
- Bowman, J. L., D. R. Smyth and E. M. Meyerowitz. 1989. Genes directing flower development in *Arabidopsis*. *The Plant Cell* 1: 37-52.
- Bowman, J. L., D. R. Smith and E. M. Meyerowitz. 1991. Genetic interactions among floral homeotic genes in *Arabidopsis*. *Development* 112:1-20.

- Bradshaw, H. D. and D. W. Schemske. 2003. Allele substitution at a flower color locus produces a pollinator shift in monkeyflowers. *Nature* 426: 176-178.
- Brockington, S. F., R. Alexandre, J. Ramdial, M. J. Moore, S. Crawley, A. Dhingra, K. Hilu et al. 2009. Phylogeny of the Caryophyllales sensu lato: Revisiting hypotheses on pollination biology and perianth differentiation in the core Caryophyllales. *International Journal of Plant Science* 170: 627-634.
- Broholm, S. K., E. Pollanen, S. Ruokolainen, S. Tahtiharju, M. Kotilainen, V. A. Albert, P. Elomaa and T. H. Teeri. 2010. Functional characterization of B class MADS-box transcription factors in *Gerbera hybrida*. *Journal of Experimental Botany* 61: 75-85.
- Bruneau, A. 1997. Evolution and homology of bird pollination syndromes in *Erythrina* (Leguminosae). *American Journal of Botany* 84: 54-71.
- Brunet, J. 2009. Pollinators of the Rocky mountain columbine: temporal variation, functional groups and associations with floral traits. *Annals of Botany* 103: 1567-1578.
- Campbell, D. R. 1996. Evolution of floral traits in hermaphroditic plant: field measurements of heritabilities and genetic correlations. *Evolution* 50: 1442-1453.
- Carpenter, R. and E. S. Coen. 1990. Floral homeotic mutations produced by transposon-mutagenesis in *Antirrhinum majus*. *Genes and Development* 4: 1483-1493.
- Castellanos, M. C., P. Wilson and J. D. Thomson. 2004. 'Anti-bee' and 'pro-bird' changes during the evolution of hummingbird pollination in *Penstemon* flowers. *Journal of Evolutionary Biology* 17: 876-885.
- Chittka, L. and N. E. Raine. 2006. Recognition of flowers by pollinators. *Current Opinion in Plant Biology* 9: 428-435.
- Christensen, K. and H. Hansen. 1998. SEM-studies of epidermal patterns in the angiosperms. *Opera Botanica* 135: 1-91.

- Coen, E. S. and E. M. Meyerowitz. 1991. The war of the whorls: genetic interactions controlling flower development. *Nature* 353: 31-37.
- Coen, E. S., S. Doyle, J. M. Romero, R. Elliot, R. Magrath and R. Carpenter. 1991. Homeotic genes controlling flower development in *Antirrhinum*. *Development* 113: 149-155.
- Comba, L., S. A. Corbet, H. Hunt et al. 2000. The role of genes influencing the corolla in pollination of *Antirrhinum majus*. *Plant, Cell and Environment* 23: 639-647.
- Crepet, W. L. 1984. Advanced (constant) insect pollination mechanisms: pattern of evolution and implications vis-a-vis angiosperm diversity. *Annals of the Missouri Botanical Garden* 71: 607-630.
- Cronk, Q. and I. Ojeda. 2008. Bird-pollinated flowers in an evolutionary and molecular context. *Journal of Experimental Biology* 59: 715-727.
- de Martino, G., I. Pan, E. Emmanuel, A. Levy and V. F. Irish. 2006. Functional analyses of two tomato *APETALA3* genes demonstrate diversification in their roles in regulating floral development. *The Plant Cell* 18: 1833-1845.
- Di Stilio, V. S., C. Martin, A. F. Schulfer and C. F. Connelly. 2009. An ortholog of *MIXTA-like2* controls epidermal cell shape in flowers of *Thalictrum*. *New Phytologist* 183: 718-728.
- Drea, S., L. C. Hileman, G. de Martino and V. F. Irish. 2007. Functional analyses of genetic pathways controlling petal specification in poppy. *Development* 134: 4157-4166.
- Duchen, P. and S. S. Renner. 2010. The evolution of *Cayaponia* (Cucurbitaceae): repeated shifts from bat to bee pollination and long-distance dispersal to Africa 2-5 million years ago. *American Journal of Botany* 97: 1129-1141.

- Dudash, M. R., C. Hassler, P. M. Stevens et al. 2011. Experimental floral and inflorescence trait manipulations affect pollinator preference and function in a hummingbird-pollinated plant. *American Journal of Botany* 98: 275-282.
- Edgar, R. C. 2004. MUSCLE: multiple sequence alignment with high accuracy and high throughput. *Nucleic Acid Research* 32:1792-1797.
- Elisens, W. J. 1992. Genetic divergence in *Galvezia* (Scrophulariaceae): evolutionary and biogeographic relationships among South American and Galapagos species. *American Journal of Botany* 79: 198-206.
- Elisens, W. J. 1986. Pollen morphology and systematic relationships among New World species in tribe Antirrhineae (Scrophulariaceae). *American Journal of Botany* 73: 1298-1311.
- Elisens, W. J. 1985. Monograph of the Maurandyinae (Scrophulariaceae- Antirrhineae). *Systematic Botany Monographs* 5: 1-97.
- Elisens, W. J. and D. J. Crawford. 1988. Genetic variation and differentiation in the genus *Mabrya* (Scrophulariaceae- Antirrhineae): systematic and evolutionary inferences. *American Journal of Botany* 75: 85-96.
- Elisens, W. J. and C. E. Freeman. 1988. Floral nectar sugar composition and pollinator type among new world genera in tribe Antirrhineae (Scrophulariaceae). *American Journal of Botany* 75: 971-978.
- Ellis, A. G. and S. D. Johnson. 2009. The evolution of floral variation without pollinator shifts in *Gorteria diffusa* (Asteraceae). *American Journal of Botany* 96: 793-801.
- Endress, P. K. 2011. Evolutionary diversification of the flowers in angiosperms. *American Journal of Botany* 98: 370-396.
- Fenster, C. B., W. S. Armbruster, P. Wilson et al. 2004. Pollination syndromes and floral specialization. *Annual Review of Ecology and Evolutionary Systematics* 35: 375-403.

- Ferrario, S., R. G. H. Immink and G. C. Angenent. 2004. Conservation and diversity in flower land. *Current Opinion in Plant Biology* 7: 84-91.
- Friedman, J. and S. C. Barret. 2008. A phylogenetic analysis of the evolution of wind pollination in the angiosperms. *International Journal of Plant Science* 169: 49-58.
- Fulton, M. and S. A. Hodges. 1999. Floral isolation between *Aquilegia formosa* and *Aquilegia pubescens*. *Proceedings of the Royal Society of London Biological Sciences* 266: 2247-2252.
- Geuten, K., A. Becker, K. Kaufmann, et al. 2006. Petaloidy and petal identity MADS-box genes in the balsaminoid genera *Impatiens* and *Marcgravia*. *Plant Journal* 47: 501-518.
- Ghebrehwet, M., B. Bremer and M. Thulin. 2000. Phylogeny of the tribe Antirrhineae (Scrophulariaceae) based on morphological and *ndhF* sequence data. *Plant systematics and evolution* 220: 223-239.
- Glover, B. 2007. Understanding flowers & flowering: an integrated approach. Oxford University Press, Oxford, New York, USA.
- Glover, B. J. and C. Martin. 1998. The role of petal cell shape and pigmentation in pollination success in *Antirrhinum majus*. *Heredity* 80: 778-784.
- Glover, B. J., M. Perez-Rodriguez and C. Martin. 1998. Development of several epidermal cell types can be specified by the same MYB-related plant transcription factor. *Development* 125: 3497-3508.
- Goldblatt, P., J. C. Manning and P. Bernhardt. 2001. Radiation of pollination systems in *Gladiolus* (Iridaceae: Crocoideae) in Southern Africa. *Annals of the Missouri Botanical Garden* 88: 713-734.

- Gorton, H. L. and T. C. Vogelmann. 1996. Effects of epidermal cell shape and pigmentation on optical properties of *Antirrhinum* petals at visible and ultraviolet wavelengths. *Plant Physiology* 112: 879-888.
- Goto, K. and E. M. Meyerowitz. 1994. Function and regulation of the *Arabidopsis* floral homeotic gene *PISTILLATA*. *Genes and Development* 8: 1548-1560.
- Grant, V. and K. A. Grant. 1965. Flower pollination in the Phlox family. Columbia University Press, New York, USA.
- Harvey, P. H. and M. D. Pagel. 1991. The comparative method in Evolutionary Biology. In: *The comparative method in Evolutionary Biology*. Oxford University Press, Oxford, UK.
- Hileman, L. C., J. F. Sundstrom, A. Litt, M. Chen, T. Shumba and V. F. Irish. 2006. Molecular and phylogenetic analyses of the MADS-box gene family in tomato. *Molecular Biology and Evolution* 23: 2245-2258.
- Hileman, L. C. and V. F. Irish. 2009. More is better: the uses of developmental genetic data to reconstruct perianth evolution. *American Journal of Botany* 96: 83-95.
- Hoballah, M. E., T. Gübitz, J. Stuurman et al. 2007. Single gene-mediated shift in pollinator attraction in *Petunia*. *The Plant Cell* 19: 779-790.
- Howarth, D. G. and D. A. Baum. 2005. Genealogical evidence of homoploid hybrid speciation in an adaptive radiation of *Scaevola* (Goodeniaceae) in the Hawaiian islands. *Evolution* 59: 948-961.
- Huelsenbeck, J. P. and F. Ronquist. 2001. MRBAYES: bayesian inference of phylogenetic trees. *Bioinformatics* 17: 754-755.
- Irish, V. F. 2009. Evolution of petal identity. *Journal of Experimental Biology* 60: 2517-2527.

- Jack, T., L. L. Brockman and E. M. Meyerowitz. 1992. The homeotic gene *APETALA3* of *Arabidopsis thaliana* encodes a MADS box and is expressed in petals and stamens. *Cell* 68: 683-697.
- Jackson, D. 1991. *in situ* hybridization in plants. *Molecular Plant Pathology: A Practical Approach* 1: 163-174.
- Jaffe, F. W., A. Tattersall and B. J. Glover. 2007. A truncated MYB transcription factor from *Antirrhinum majus* regulates epidermal cell outgrowth. *Journal of Experimental Botany* 58: 1515-1524.
- Jaramillo, M. A. and E. M. Kramer. 2004. *APETALA3* and *PISTILLATA* homologs exhibit novel expression patterns in the unique perianth of *Aristolochia* (Aristolochiaceae). *Evolution & Development* 6: 449-458.
- Jaramillo, M. A. and E. M. Kramer. 2007. Molecular evolution of the petal and stamen identity genes, *APETALA3* and *PISTILLATA*, after petal loss in the Piperales. *Molecular Phylogenetics And Evolution* 44: 598-609.
- Johnson, S. D., T. J. Edwards, C. Carbutt and C. Potgieter. 2002. Specialization for hawkmoth and long-proboscid fly pollination in *Zaluzianskya* section *Nycterinia* (Scrophulariaceae). *Botanical Journal of the Linnean Society* 138: 17-27.
- Johnson, S. D., H. P. Linde and K. E. Steiner. 1998. Phylogeny and radiation of pollination systems in *Disa* (Orchidaceae). *American Journal of Botany* 85: 402-411.
- Jones, K. N. and J. S. Reithel. 2001. Pollinator-mediated selection on a flower color polymorphisms in experimental populations of *Antirrhinum* (Scrophulariaceae). *American Journal of Botany* 88: 447-454.
- Kang, H. G., J. S. Jeon, S. Lee and G. H. An. 1998. Identification of class B and class C floral organ identity genes from rice plants. *Plant Molecular Biology* 38: 1021-1029.

- Kanno A., H. Saeki, T. Kameya, H. Saedler and G. Theissen. 2003. Heterotopic expression of class B floral homeotic genes supports a modified ABC model for tulip (*Tulipa gesneriana*). *Plant Molecular Biology* 52: 831-841.
- Kay, K. M., P. A. Reeves, R. G. Olmstead and D. W. Schemske. 2005. Rapid speciation and the evolution of hummingbird pollination in neotropical *Costus* subgenus *Costus* (Costaceae): evidence from nrDNA ITS and ETS sequences. *American Journal of Botany* 92: 1899-1910.
- Kay, K. M. and D. W. Schemske. 2003. Pollinator assemblages and visitation rates for 11 species of neotropical *Costus* (Costaceae). *Biotropica* 35: 198-207.
- Kay, Q. O. N., H. S. Daoud and C. H. Striton. 1981. Pigment distribution, light reflection and cell structure in petals. *Botanical Journal of the Linnean Society* 83: 57-84.
- Kevan, P. G. and M. A. Lane. 1985. Flower petal microtexture is a tactile cue for bees. *Proceedings of the National Academy of Sciences of the United States of America* 82: 4750-4752.
- Kim, S. Y., P. Y. Yun, T. Fukuda, T. Ochiai, J. Yokoyama, T. Kameya and A. Kanno. 2007. Expression of a *DEFICIENS*-like gene correlates with the differentiation between sepal and petal in the orchid, *Habenaria radiata* (Orchidaceae). *Plant Science* 172: 319-326.
- Kim, S., J. Koh, M. Yoo, et al. 2005. Expression of floral MADS-box genes in basal angiosperms: implications for the evolution of floral regulators. *The Plant Journal* 43: 724-744.
- Kramer, E. M. 2007. Understanding the genetic basis of floral diversity. *Bioscience* 57: 479-487.
- Kramer, E. M., V. S. DiStilio and P. M. Schluter. 2003. Complex patterns of gene duplication in the *APETALA3* and *PISTILLATA* lineages of the Ranunculaceae. *International Journal of Plant Sciences* 164: 1-11.

- Kramer, E. M., L. Holappa, B. Gould, M. A. Jaramillo, D. Setnikov and P. M. Santiago. 2007. Elaboration of B gene function to include the identity of novel floral organs in the lower eudicot *Aquilegia*. *The Plant Cell* 19: 750-766.
- Krizek, B. A. and E. M. Meyerowitz. 1996. the *Arabidopsis* homeotic genes *APETALA3* and *PISTILLATA* are sufficient to provide the B class organ identity function. *Development* 122: 11-22.
- Lara, C. and J. F. Ornelas. 2008. Pollination ecology of *Penstemon roseus* (Plantaginaceae), an endemic perennial shifted toward hummingbird specialization? *Plant Systematics and Evolution* 271: 223-237.
- Litt, A. and E. M. Kramer. 2010. the ABC model and the diversification of floral organ identity. *Seminars In Cell and Developmental Biology* 21: 129-137.
- Little, R. J. 1983. A review of floral food deception mimics with comments on floral mutualism. In: Jones C.E. , Little R.J. (eds.) Handbook of experimental pollination biology. Scientific and Academic Editions, Van Nostrand Reinhold Company.: New York, 294-309.
- Liu, Y., N. Nakayama, M. Schiff, A. Litt, V. F. Irish and S. P. Dinesh-Kumar. 2004. Virus induced gene silencing of a *DEFICIENS* ortholog in *Nicotiana benthamiana*. *Plant Molecular Biology* 54:701-711.
- Machado, A., Y. Wu, Y. Yang et al. 2009. The MYB transcription factor GhMYB25 regulates early fibre and trichome development. *The Plant Journal* 59: 52-62.
- Maddison, D. R. and W. P. Maddison. 2005. Macclade 4: analysis of phylogeny and character evolution version 4.08. Sinauer Associates, Sunderland, Massachusetts.
- Magallon, S., P. R. Crane and P.S. Herendeen. 1999. Phylogenetic pattern, diversity, diversification of eudicots. *Annals of the Missouri Botanical Garden* 86: 297-372.

- Martin, C., K. Bhatt, K. Baumann et al. 2002. The mechanics of cell fate determination in petals. *Philosophical Transactions of the Royal Society of London Biological Sciences* 357: 809-813.
- Martin, N. H., Y. Sapir and M. L. Arnold. 2008. Irises: pollination syndromes and pollinator preferences. *Evolution* 62: 740-752.
- Maturen, N. M. 2008. *Genetic analysis of the evolution of petaloid bracts in dogwoods*. Ph.D. dissertation, University of Michigan, Ann Arbor, Michigan, USA.
- Nakamura, T., T. Fukuda, M. Nakano, M. Hasebe, T. Kameya and A. Kanno. 2005. The modified ABC model explains the development of the petaloid perianth of *Agapanthus praecox* ssp. *orientalis* (Agapanthaceae) flowers. *Plant Molecular Biology* 58: 435-445.
- Noda, K., B. J. Glover, P. Linstead and C. Martin. 1994. Flower color intensity depends on specialized cell-shape controlled by a MYB-related transcription factor. *Nature* 369: 661-664.
- Ojeda, I., J. Francisco-Ortega and Q.C.B. Cronk. 2009. Evolution of petal epidermal micromorphology in Leguminosae and its use as a marker of petal identity. *Annals of Botany* 104: 1099-1110.
- Park, J. H., Y. Ishikawa, R. Oshida, A. Kanno and T. Kameya. 2003. Expression of *AoDEF*, a B-functional MADS-box gene, in stamens and inner tepals of the dioecious species *Asparagus officinalis* L. *Plant Molecular Biology* 51: 867-875.
- Park, J. H., Y. Ishikawa, T. Ochiai, A. Kanno and T. Kameya. 2004. Two *GLOBOSA*-like genes are expressed in second and third whorls of homochlamydeous flowers in *Asparagus officinalis* L. *Plant Cell Physiology* 45: 325-332.

- Perez, F., M. T. K. Arroyo, R. Medel and M. A. Hershkovitz. 2006. Ancestral reconstruction of flower morphology and pollination systems in *Schizanthus* (Solanaceae). *American Journal of Botany* 97: 1029-1038.
- Perez-Rodriguez, M., F. W. Jaffe, E. Butelli, B. J. Glover and C. Martin. 2005. Development of three different cell types is associated with the activity of a specific MYB transcription factor in the ventral petal of *Antirrhinum majus* flowers. *Development* 132: 359-370.
- Posada, D. 2008. jModelTest: Phylogenetic Model Averaging. *Molecular Biology and Evolution* 25: 1253-1256.
- Prasad, K. and U. Vijayraghavan. 2003. Double-stranded RNA interference of rice *PI/GLO* paralog, *OsMADS2*, uncovers its second-whorl-specific function in floral organ patterning. *Genetics* 165: 2301-2305.
- Prasad, K., P. Sriram, C. S. Kumar, K. Kushalappa and U. Vijayraghavan. 2001. Ectopic expression of rice *OsMADS1* reveals a role in specifying the lemma and palea, grass floral organs analogous to sepals. *Development Genes and Evolution* 211: 281-290.
- Preston, J. C. and E. A. Kellogg. 2007. Conservation and divergence of *APETALA1/FRUITFULL*-like gene function in grasses: evidence from gene expression analyses. *The Plant Journal* 52: 69-81.
- Rasmussen, D. A., E. M. Kramer and E. A. Zimmer. 2009. One size fits all? Molecular evidence for a commonly inherited petal identity program in ranunculales. *American Journal Of Botany* 96: 96-109.
- Rausher, M.D. 2008. Evolutionary transitions in floral color. *International Journal of Plant Science* 169: 7-21.

- Rijpkema, A. S., S. Royaert, J. Zethof, G. van der Weerden, T. Gerates and M. Vandenbussche. 2006. Analysis of the *Petunia TM6* MADS box gene reveals functional divergence within the *DEF/AP3* lineage. *The Plant Cell* 18:1819-1832.
- Ronquist, F. and J. P. Huelsenbeck. 2003. MRBAYES 3: Bayesian phylogenetic inference under mixed models. *Bioinformatics* 19: 1572-1574.
- Ronse De Craene, L. P. 2008. Homology and evolution of petals in the core eudicots. *Systematic Botany* 33: 301-325.
- Ronse De Craene, L. P. 2007. Are petals sterile stamens or bracts? The origin and evolution of petals in the core eudicots. *Annals Of Botany* 100: 621-630.
- Sandring, S. and J. Ågren. 2009. Pollinator-mediated selection on floral display and flowering time in the perennial herb *Arabidopsis lyrata*. *Evolution* 63: 1292-1300.
- Schemske, D.W. and H. D. Bradshaw, Jr. 1999. Pollinator preference and the evolution of floral traits in monkeyflowers (*Mimulus*). *Proceedings of the National Academy of Sciences* 96: 11910-11915.
- Schiestl, F. P., F. K. Huber and J. M Gomez. 2011. Phenotypic selection on floral scent: trade-off between attraction and deterrence? *Evolutionary Ecology* 25: 237-248.
- Schlumpberger, B. O., A. A. Cocucci, M. More et al. 2009. Extreme variation in floral characters and its consequences for pollinator attraction among populations of an Andean cactus. *Annals of Botany* 103: 1489-1500.
- Schwarz-Sommer, Z., P. Huijser, W. Nacken, H. Saedler and H. Sommer. 1990. Genetic control of flower development by homeotic genes in *Antirrhinum majus*. *Science* 250: 931-936.
- Sletvold, N., J. M. Grindeland and J. Ågren. 2010. Pollinator-mediated selection on floral display, spur length and flower phenology in the deceptive orchid *Dactylorhiza lapponica*. *New Phytologist* 188: 385-392.

- Smith, S. D. 2010. Using phylogenetics to detect pollinator-mediated floral evolution. *New Phytologist* 188: 354-363.
- Smith, S. D., C. Ane and D. A. Baum. 2008. The role of pollinator shifts in the floral diversification of *Iochroma* (Solanaceae). *Evolution* 62: 793-806.
- Soltis, P. S., S. F. Brockington, M. J. Yoo, A. Piedrahita, M. Latvis, M. J. Moore, A. S. Chanderbali and D. E. Soltis. 2009. Floral variation and floral genetics in basal angiosperms. *American Journal Of Botany* 96: 110-128.
- Sommer, H., J. P. Beltran, P. Huijser, H. Pape, W. E. Lonig, H. Saedler and Z. Schwarz-Sommer. 1990. *DEFICIENS*, a homeotic gene involved in the control of flower morphogenesis in *Antirrhinum majus*: the protein shows homology to transcription factors. *Embo Journal* 9: 605-613.
- Stebbins, G.L. 1970. Adaptive radiation of reproductive characteristics in angiosperms. I: Pollination mechanisms. *Annual Review of Ecological Systematics* 1: 307-326.
- Sutton, D. A. 1988. A revision of the tribe Antirrhineae. Oxford University Press, New York, USA.
- Swofford, D. L. 2002. PAUP*. Phylogenetic analysis using parsimony (*and other methods). Version 4. Sinauer Associates, Sunderland, Massachusetts, USA.
- Thompson, D. M. 1988. Systematics of *Antirrhinum* (Scrophulariaceae) in the New World. *Systematic Botany Monographs*: 1-142.
- Thomson, J. D. and B. Thomson. 1992. Pollen presentation and viability schedules in animal-pollination plants: consequences for reproductive success. In: *Ecology and Evolution of Plant Reproduction* (R. Wyatt, ed.). Chapman and Hall, New York, USA, pp 1-24.

- Tripp, E. A. and P. S. Manos. 2008. Is floral specialization an evolutionary dead-end? Pollination system transitions in *Ruellia* (Acanthaceae). *Evolution* 62: 1712-1737.
- Trobner, W., L. Ramirez, P. Motte, I. Hue, P. Huijser, W.E. Lonng, H. Saedler, et al. 1992. *globosa* - a homeotic gene which interacts with *deficiens* in the control of *Antirrhinum* floral organogenesis. *Embo Journal* 11: 4693-4704.
- Tzeng, T. Y. and C. H. Yang. 2001. A MADS box gene from lily (*Lilium longiflorum*) is sufficient to generate dominant negative mutation by interacting with *PISTILLATA (PI)* in *Arabidopsis thaliana*. *Plant Cell Physiology* 42: 1156-1168.
- van Houwelingen, A., E. Souer, K. Spelt et al. 1998. Analysis of flower pigmentation mutants generated by random transposon mutagenesis in *Petunia x hybrida*. *The Plant Journal* 31: 39-50.
- Vandenbussche, M., J. Zethof, S. Royaert, K. Weterings and T. Gerats. 2004. The duplicated B-class heterodimer model: whorl-specific effects and complex genetic interactions in *Petunia x hybrida* flower development. *The Plant Cell* 16: 741-754.
- Vargas, P., J. A. Rossello, R. Oyama and J. Guemes. 2004. Molecular evidence for naturalness of genera in the tribe Antirrhineae (Scrophulariaceae) and three independent evolutionary lineages from the new world and the old. *Plant Systematics and Evolution* 249: 151-172.
- Waser, N.M. 2006. Specialization and generalization in plant-pollinator interactions: a historical perspective. In: Waser, N.M., J. Ollerton, eds. *Plant-pollinator interactions from specialization to generalization*. University of Chicago Press, Chicago, IL: 3-17.
- Weiss, D. 2000. Regulation of flower pigmentation and growth: multiple signaling pathways control anthocyanin synthesis in expanding petals. *Physiologia Plantarum* 110: 152-157.

- Whipple, C. J., P. Ciceri, C. M. Padilla, B. A. Ambrose, S. L. Bandong and R. J. Schmidt. 2004. Conservation of B-class floral homeotic gene function between maize and *Arabidopsis*. *Development* 131: 6083-6091.
- Whitney, H. M., L. Chittka, T. J. A. Bruce and B. J. Glover. 2009. Conical epidermal cells allow bees to grip flowers and increase foraging efficiency. *Current Biology* 19: 948-953.
- Whitney, H. M. and B. J. Glover. 2007. Morphology and development of floral features recognised by pollinators. *Arthropod-Plant Interactions* 1: 147-158.
- Whittall, J.B. and S. A. Hodges. 2007. Pollinator shift drive increasingly long nectar spurs in columbine flowers. *Nature* 44: 706-710.
- Whittall, J. B., C. Voelckel, D. J. Kliebenstein and S. A. Hodges. 2006. Convergence, constraint and the role of gene expression during adaptive radiation: floral anthocyanins in *Aquilegia*. *Molecular Ecology* 15: 4645-4657.
- Wikstrom, N., V. Savolainen and M. W. Chase. 2001. Evolution of the angiosperms: calibrating the family tree. *Proceedings of the Royal Society of London Biological Sciences* 268: 2211-2220.
- Wilson, P., A. D. Wolfe, W. S. Armbruster and J. D. Thomson. 2007. Constrained lability in floral evolution: counting convergent origins of hummingbird pollination in *Penstemon* and *Keckiella*. *New Phytologist* 176: 883-890.
- Wu, H., H. Su and J. Hu. 2007. The identification of A-, B-, C- and E-class MADS-box genes and implications for perianth evolution in the basal eudicot *Trochodendron aralioides* (Trochodendraceae). *International Journal Of Plant Sciences* 168(6): 775-799.
- Xiao, H., Y. Wang, D. F. Liu, W. M. Wang, X. B. Li, X. F. Zhao, J. C. Xu et al. 2003. Functional analysis of the rice *AP3* homologue *OsMADS16* by RNA interference. *Plant Molecular Biology* 52:957-966.

- Yang, Y., L. Fanning and T. J. 2003. The K domain mediates heterodimerization of the *Arabidopsis* floral organ identity proteins, *APETALA3* and *PISTILLATA*. *The Plant Journal* 33: 47-59.
- Yoo, M., P. S. Soltis and D. E. Soltis. 2010. Expression of floral MADS-box genes in two divergent water lilies: Nymphaeales and *Nelumbo*. *International Journal Of Plant Sciences* 171: 121-146.
- Zanis, M. J., P. S. Soltis, Y. L. Qiu, E. Zimmer and D. E. Soltis. 2003. Phylogenetic analyses and perianth evolution in basal angiosperms. *Annals Of The Missouri Botanical Garden* 90: 129-150.
- Zhang, W., Q. Xiang, D. T. Thomas, B. M. Wiegmann, M. W. Frohlich and D. E. Soltis. 2008. Molecular evolution of *PISTILLATA*-like genes in the dogwood genus *Cornus* (Cornaceae). *Molecular Phylogenetics and Evolution* 47: 175-195.
- Zwickl, D. J. 2006. *Genetic algorithm approaches for the phylogenetic analysis of large biological sequence datasets under the maximum likelihood criterion*. Ph.D. Dissertation, The University Of Texas, Austin, Texas, USA.

Appendix 1. GenBank Accession numbers

Table of downloaded GenBank gene sequences of *DEFICIENS* and *GLOBOSA* from a wide range of taxa used for phylogenetic analyses.

Taxon; *DEF/GLO* GenBank accession.

Antirrhinum majus L.; AmDEF X52023, AmGLO AB516403. *Arabidopsis thaliana* L.; AtAP3 NM_115294, AtPI NM_122031. *Brassica napus* L.; BnAP3 DQ372719. *Camellia japonica* L.; GQ141126. *Chelone glabra* L.; CgDEF AY524008. *Diospyros digyna* Jacq.; DdGLO GQ141136. *Lycopersicon esculentum* L.; LeTAP3 DQ674532, LeTPI DQ674531. *Mimulus guttatus* DC.; MgDEFA AY524012, MgDEFB AY524020. *Mimulus kelloggi* (Curran ex Greene) Curran ex A. Gray; MkDEF AY530545. *Misopates orontium* (L.) Raf.; MoDEF AM162207, MoGLO Am162211. *Napoleona vogelii* Hook. & Planch; NvGLO GQ141117. *Papaver somniferum* L.; PsAP3-1 EF071993, PsAP3-2 EF071992, PsPI-1 EF071994, PsPI-2 EF071995. *Paulownia tomentosa* (Thunb.) Steud.; PtDEF AY524018. *Petunia hybrida* Juss.; PhDEF DQ539416. *Phlox paniculata* L.; PpDEF GQ141172, GQ141129. *Rhodochiton atrosanguineum* L.; RaDEF XXXXXXXX, RaGLO XXXXXXXX. *Saxifraga caryana* L.; ScAP3 DQ479367. *Syringa vulgaris* L.; SvAP3 DQ479367, SvPI-1 AF052861. *Torenia fournieri* L.; TfGLO AB359952.

Appendix 2. GenBank accession numbers for *MIXTA-LIKE* genes

Table of downloaded and newly sequenced GenBank gene sequences of *MIXTA*, *MIXTA-LIKE 1*, *MIXTA-LIKE 2*, and *MIXTA-LIKE 3* genes in members of Antirrhineae (Plantaginaceae).

Taxon; MIX/ML1/ML2/ML3 GenBank accession.

Anarrhinum bellidifolium L.; AbMIX XXXXXXXXX, AbML2 XXXXXXXXX, AbML3 XXXXXXXXX. *Antirrhinum majus* L.; AmMIX X79108, AmML1 AJ006292, AmML2 AY821655, AmML3 AY661654. *Asarina procumbens* Miller; ApMIX XXXXXXXXX, ApML1 XXXXXXXXX, ApML2 XXXXXXXXX, ApML3 XXXXXXXXX. *Cymbalaria muralis* P. Gaertner, B. Meyer & Scherb.; CmMIX XXXXXXXXX, CmML1 XXXXXXXXX, CmML2 XXXXXXXXX, CmML3 XXXXXXXXX. *Galvezia fruticosa* J.F. Gmelin; GfMIX XXXXXXXXX, GfML1 XXXXXXXXX, GfML2 XXXXXXXXX, GfML3. *Gambelia speciosa* Nutt.; GsMIX XXXXXXXXX, GsML1 XXXXXXXXX, GsML2 XXXXXXXXX, GsML3 XXXXXXXXX. *Kickxia elatine* (L.) Dumort.; KeMIX XXXXXXXXX, KeML1 XXXXXXXXX, KeML3 XXXXXXXXX. *Linaria vulgaris* Miller; LvMIX XXXXXXXXX, LvML1 XXXXXXXXX, LvML2 XXXXXXXXX, LvML3 XXXXXXXXX. *Lophospermum erubescens* D. Don in Sweet; LeMIX XXXXXXXXX, LeML1 XXXXXXXXX, LeML2 XXXXXXXXX, LeML3 XXXXXXXXX. *Lophospermum purpusii* (T.S. Brandege) Rothm.; LpMIX XXXXXXXXX, LpML1 XXXXXXXXX, LpML2 XXXXXXXXX, LpML3 XXXXXXXXX. *Mabrya acerifolia* (Pennell) Elisens; MaMIX XXXXXXXXX, MaML1 XXXXXXXXX, MaML2 XXXXXXXXX, MaML3 XXXXXXXXX. *Mabrya rosei* (Munz) Elisens; MrMIX XXXXXXXXX, MrML1 XXXXXXXXX, MrML2 XXXXXXXXX, MrML3 XXXXXXXXX. *Maurandella antirrhiniflora* (Willd.) Rothm.; MaMIX XXXXXXXXX, MaML1 XXXXXXXXX, MaML2 XXXXXXXXX, MaML3 XXXXXXXXX. *Maurandya scandens* (Cav.) Pers.; MsMIX XXXXXXXXX, MsML1 XXXXXXXXX, MsML2 XXXXXXXXX, MsML3 XXXXXXXXX. *Misopates orontium* (L.) Rafin.; MoMIX XXXXXXXXX, MoML1 XXXXXXXXX,

MoML3 XXXXXXXXX. *Rhodochiton atrosanguineum* (Zucc.) Rothm.; RaMIX XXXXXXXXX,
RaML1 XXXXXXXXX, RaML2 XXXXXXXXX, RaML3 XXXXXXXXX. *Sairocarpus*
coulterianum (A. DC.) D. A. Sutton; ScMIX XXXXXXXXX, ScML1 XXXXXXXXX, ScML2
XXXXXXXXXX, ScML3 XXXXXXXXX.